Politecnico di Torino

Avio Aero
a GE Aerospace company

LPT blade Sensitivity of the Boundary Condition at the interlocking and impact on flutter stability

Master's degree in aerospace engineering, a.a. 2023/2024

Department of Mechanics and Aerospace, DIMEAS.
Master's degree Thesis

Professors
Prof.Christian Maria Firrone

Candidate
Francesca Ingrande

Tutor
Eng.Antonio Giuseppe D'Ettole

Abstract

Today a crucial objective of the aerospace industry is to realize lighter blades with a lower environmental impact. To pursue these objectives, it is necessary to find out innovative types of blades characterized by a new geometry feature and a lighter material. This thesis work is developed in collaboration with Avio Aero and its goal is to analyze aeroelastic issues of LPT blade, in particular the aim of this work is to show the impact of the different Boundary Conditions at the interlocking on the flutter stability. The entity of the contact at the interlocking must be studied, it is not possible to establish it in a deterministic way because during the blade's service life causing flutter instability it could change. In this regard, three different contact configurations at the interlocking are analyzed in this work: TIGHT, RADIAL FREE and TIP FREE. Modal Analysis and Flutter Analysis are performed for each case to understand the impact on Modeshapes, Frequency and Flutter Stability. The Modal Analysis is performed by Finite Element Method with ANSYS APDL, Flutter Analysis instead by a CFD Finite Volume Method with a non-linearized flutter solver. In this work, all the process to perform a Flutter analysis through all the theoretical knowledges of all the steps is also explained. All the results and comparisons of the analysis performed between all the cases are shown. The results shows that TIP FREE configuration is more dangerous than the other two.

Contents

List of figures

1 Introduction

1.1 E-TDCs: European Technology Development Clusters

The E-TCDs, European Technology Development Clusters, is a network operating into the research and innovation field that was launched in May 2020, with a unique model in Europe, whose members work together under one single framework agreement which defines financial provisions, Ip rules, dissemination and publications. The E-TCDs include up today 39 parties: 16 University, 7 research institutions, 4 SMEs and 12 GE affiliates. The E-TCDs include 10 different clusters, consisting of research institutions and GE Aviation teams, each of them focused on dedicated disciplines or product of GE Aviation interest,set up taking into consideration the complementarity of knowledge and operating on the basis of an Innovation Plan with the following responsibilities:

1. To monitor the innovation plan and the international scientific scenario;
2. to exploit the complementary knowledge and capability of teams;
3. to propose extension of the collaboration to other research teams;
4. to promote, where necessary, integration with SMEs;
5. to evaluate financing opportunities through participation external funded projects;
6. to manage publications and events to disseminate the results obtained;
7. to develop skills and highly specialized human resources.

This thesis work is the result of a collaboration period between GE AvioAero

and Polytechnic University of Turin. Particularly It has been studied the interaction between fluid and structure in a Low-Pressure section of an aircraft engine. The goal of the work was specifically the study of the turbine blades flutter behavior. Before describing in detail this phenomenon, in this first chapter will be illustrated the types of aircraft engines that are present nowadays on the market[1].

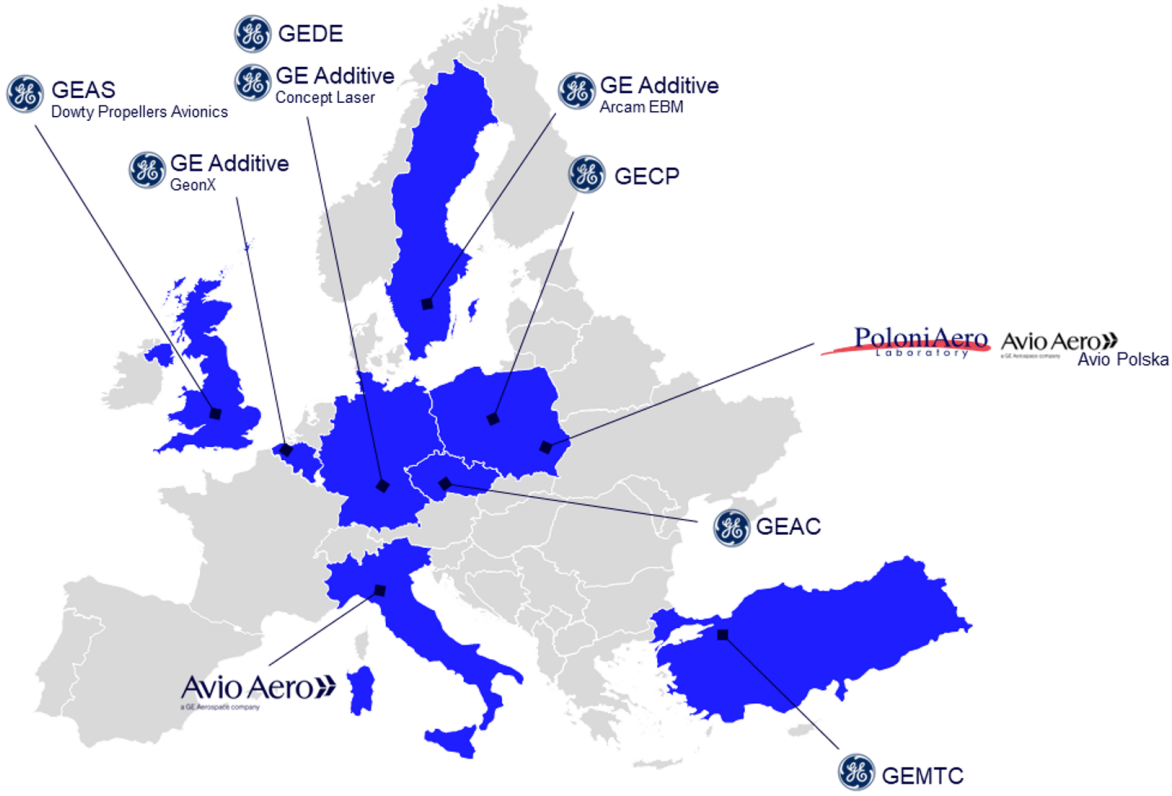

Figure 1: The E-TDCs

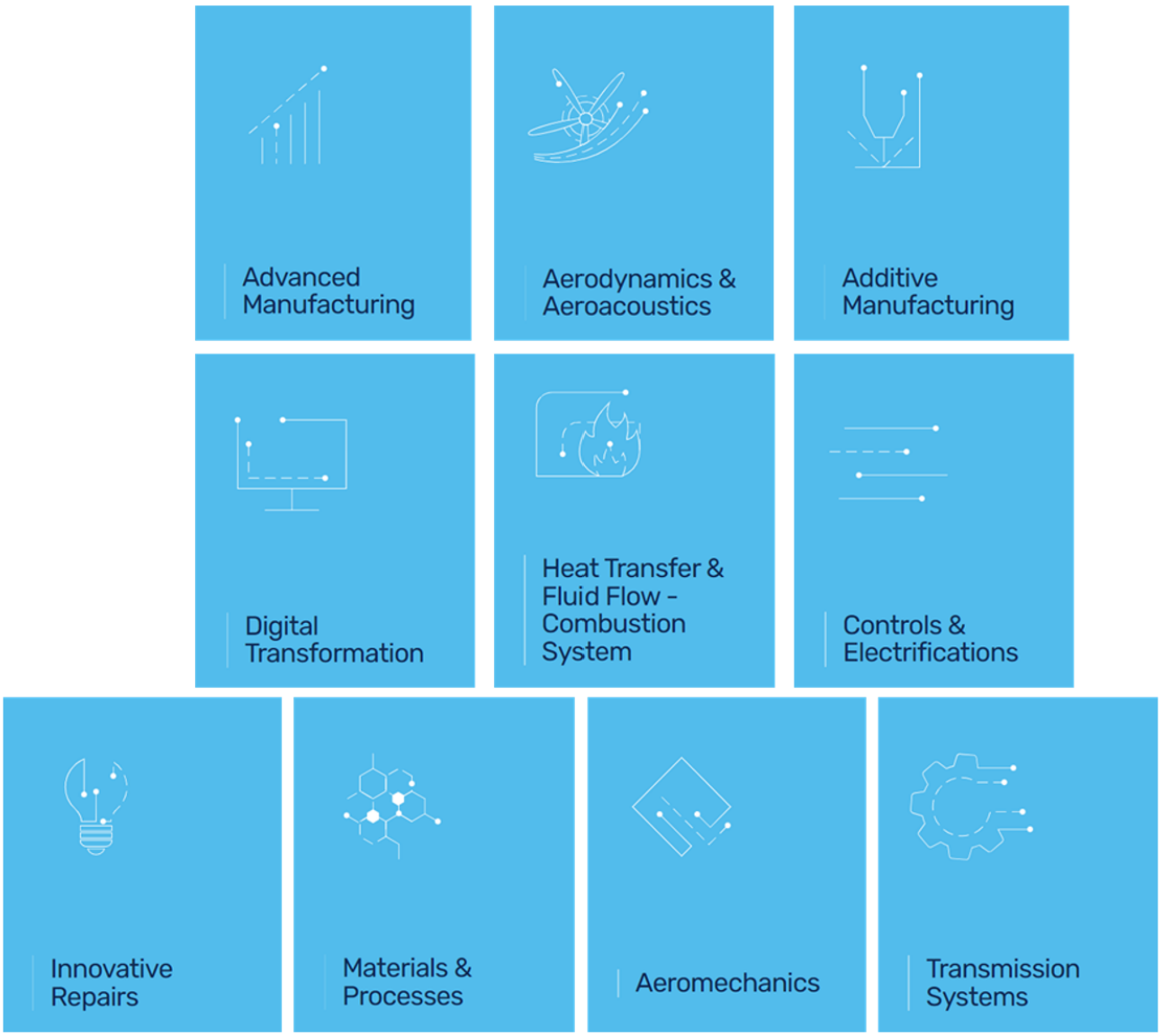

Figure 2: E-TDCs Network and Clusters

1.2 Aircraft Engines

At the beginning of the history of aviation, the concept of the aeronautical engine was very different from how we know it today, this system it consisted of a reciprocating engine that provided power to a propeller. Around 1930 it was realized that the best way to achieve high speeds was through jet propulsion systems.The jet propulsion is based on the third principle of dynamics, the flow is accelerated to generate a force , at this

force corresponds an equal and opposite force which is the thrust. A engine can be :

- *Air-breathing*:These are those engines that use air as a comburent and are therefore called this because they need air or an equivalent external fluid to function.
- *Rocket Engine*: They store the comburent on board in special tanks, they are internal combustion engines in most cases.

Focusing on the first one, all the classical airbreathing engines operate a Brayton-Joule cycle but is crucial to highlight that all engines operate this cycle in a different way. In a typical turbofan/turbojet configuration the

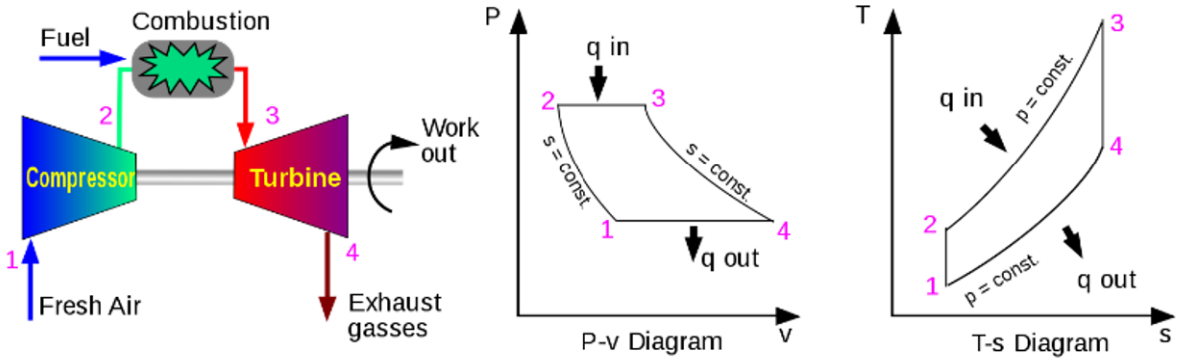

Figure 3: Joule-Brayton Cycle

gas is compressed by the compressors, then is heated in the combustor after the supply of the fuel, then it is expanded in the turbines zone generating mechanical work and then accelerated in the nozzle generating thrust.

The turbine has the task of extracting work from the fluid so as to drag the compressor, the nozzle instead converts enthalpy in to thrust. This type of engine work in a “operative line”, where the power extracted from

the fluid equals the power needed to drive the compressor.

The turboshaft has the same operative cycle except for the final part, in this configuration there is no nozzle, but there is a user, so the work extracted from the fluid is used to give power at the user. The turboprop instead is a mix of the two types of engines, because by extracting work from the fluid there are two uses of this: generate thrust in the nozzle and drive a propeller.[4]

1.2.1 Turbofan

The turbofan is a type of engine derived from the turbojet and like all the aeronautics engines its aim is to generate thrust. The typical feature of this engine is the presence of two different flows: the *cold flow* and the *hot flow*. The cold flow passes through the fan and goes out the outer nozzle, the hot flow passes through the fan too and continues through all the compressor's stages, the combustion chamber, the turbine stage and then in the inner nozzle[16].

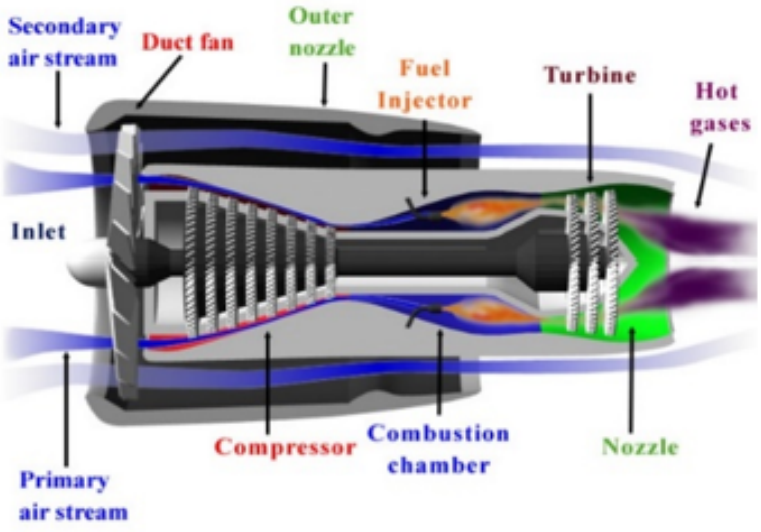

Figure 4: Turbofan Scheme

The most important parameters for the turbofan are: BPR (Bypass RATIO), η_p (Propulsion efficiency) and η_{th}(thermal efficiency). The BPR is the ratio between the mass flow rate of the bypass stream to the mass flow rate entering the core, where the first is the cold flow and the second is the hot flow.

$$BPR = \frac{\dot{m}_c}{\dot{m}_h} \tag{1}$$

where $\dot{m}_c$ is the cold flow and $\dot{m}_h$ is the hot flow. Typically, the aim is to obtain cold flow with very high propulsion efficiency and hot flow with very high thermal efficiency.

The propulsion efficiency is defined as:

$$\eta_p = \frac{P_t}{P_t + P_d} = \frac{2}{1 + \frac{v_g}{v_0}} \tag{2}$$

Where P_t is the Power of the thrust, P_d the power dissipated, v_g the gas velocity and v_0 the aircraft velocity.
The thermal efficiency is defined as:

$$\eta_t h = \frac{P_k}{P_{ch}} \tag{3}$$

Where P_k is the kinetic power and P_{ch} the chemistry power, this one could be intended like the power stored in the fuel. It is possible to define the global efficiency as:

$$\eta_g = \eta_p \eta_{th} \tag{4}$$

1.2.2 Turboshaft

The turboshaft has the role to product mechanical work which must be enslaved to a user like a propeller or a rotor. This engine extract work from the fluid thanks to the turbines and use it to drive the compressor and the user.

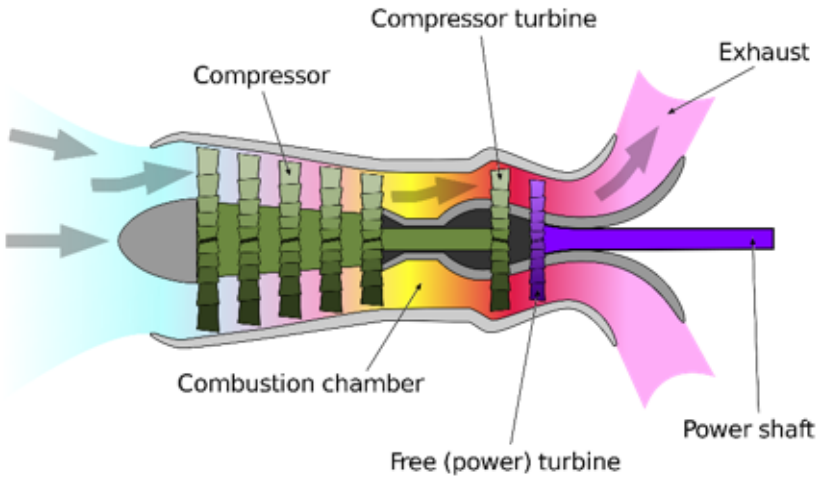

Figure 5: Turboshaft Scheme

Nowadays the most part of turboshafts are double spool machines with free turbine for power, which has the role to drive just the user. This choice is made to optimize the operation in off design conditions.

1.2.3 Turboprop

This engine is the combination of the two types of engines explained before. The thrust is produced by the propeller and the exhaust gasses both.

$$T_t = T_p + T_g \tag{5}$$

Where T_p is the thrust associated to the propeller, instead T_j contains the contribution of the jet. In the figure below there is an example of turboprop engine:

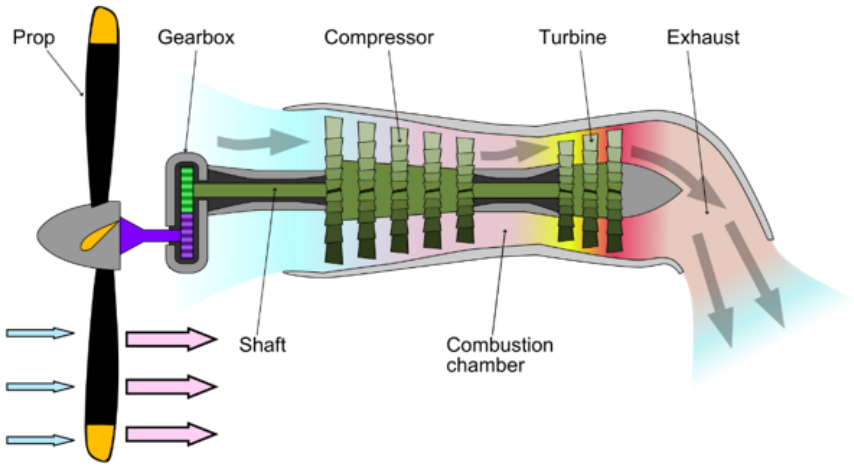

Figure 6: Turboprop Scheme

A turboprop consists of an intake,a gearbox to reduct RPM, compressor, combustor, turbine, and a propelling nozzle. The air enters throw the intake and is compressed by the compressor. Then the fuel is added to the compressed air in the combustor. The exausted gases expand through the turbine stages, generating power at the point of exhaust [17].

1.3 Low pressure turbine

Focusing on the component of interest for this thesis work, as seen before turbine drives compressor and accessories extracting kinetic energy from the expanding flow that comes from the combustion chamber. In most cases the turbines used are axial ones.

An axial turbine is a turbine in which the flow of the working fluid is parallel to the shaft, as opposed to radial turbines, where the fluid runs around a shaft, as in a watermill.

An axial turbine has a similar construction as an axial compressor, but it operates in the reverse, converting flow of the fluid into rotating mechanical energy.[12]

Each turbine stage is composed of a stator and a rotor:

- *stator*:The stator is the fixed, non-moving component and it is composed by some nozzle guide vanes which they direct the flow to obtain the angles and speed desired by design.
- *rotor*:is the rotating component, it is a bladed disk. A rotor rotates through the effect of the flow gas and obviously it is linked to the shaft.

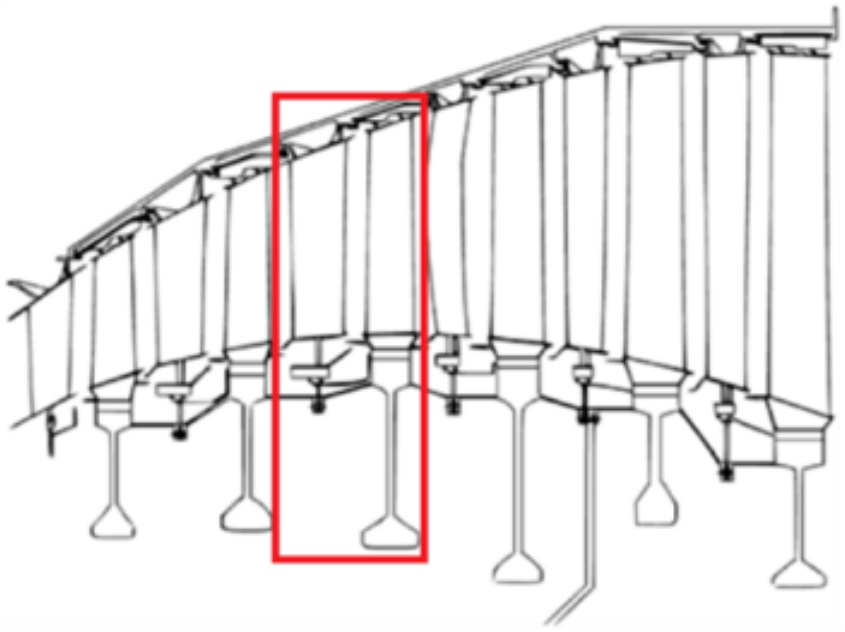

Figure 7: Stage Axial Turbine

In the picture below is shown a two-stage turbine.

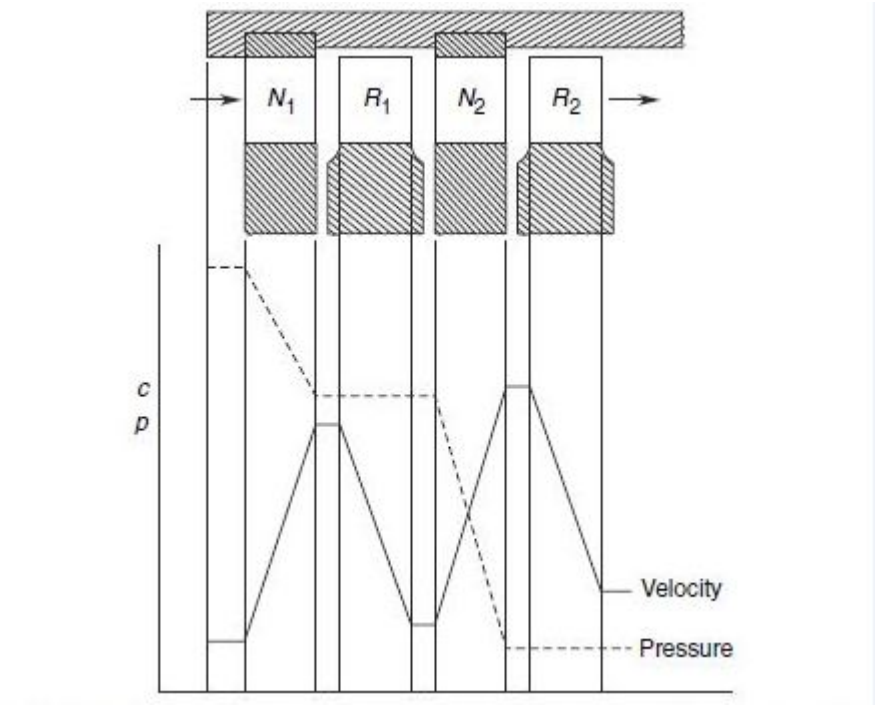

Figure 8: Two-stage Axial Turbine Scheme Example [19]

2 Rotor Dynamics

Rotor Dynamics is the study of the motion of the rotating element of any turbomachinery. Rotor component extract work from the fluid and transfers it to the shaft to provide mechanical work. This thesis work is focused on the Low-Pressure Zone of the engine, especially LPT, so all the treatment will be done by giving more emphasis to this part.

A Rotor is a Bladed component, in technical language it is spoken of bladed disk.The dynamic analysis of these components is a very challenging task for the structural designer, who must avoid resonance conditions within the operating range of the machine or, alternatively,control the vibration amplitude by introducing additional damping into the system.

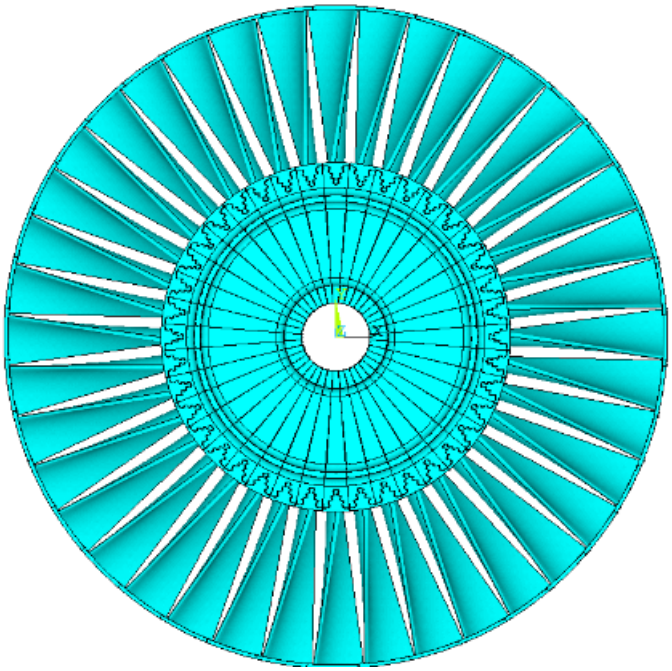

Figure 9: Bladed disk example

The works is focused on a single blade-disk complex.It is important to highlight the parts of the blade that are relevant to understand all the analysis, a blade can be *Cantilever*[1] or *Shrouded*, for this thesis we are focusing on the shrouded type:

1. **Shroud**: it is located at the tip of the blade, and it has two important roles, limit the generation of whirling structures on the tip and dump the vibrations of the structure.

2. **Airfoil**:is the surface that exchange work with fluid.

3. **Shank**:it is the part that links the blade to the disk.

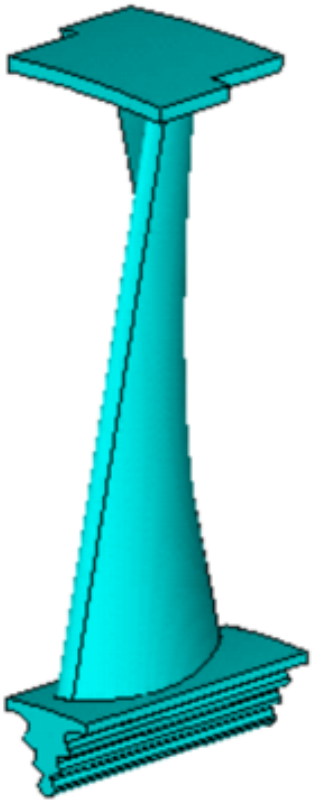

Figure 10: Dummy model of a shrouded turbine blade

[1]A blade cantilever is without any tipe of shroud, so it is composed only by airfoil and shank

In this work we are focusing on the shroud of the blade to describe the parts of interest in order to understand all the analysis done.The most important part of the shroud and of greatest interest is the **interlocking**, which is the contact surface between two consecutive blades at the tip shroud. In the picture below Figure [11] is reported a dummy model for the corporate secrecy. The other surfaces at the tip shroud are "free", so there is a GAP between the two surfaces.

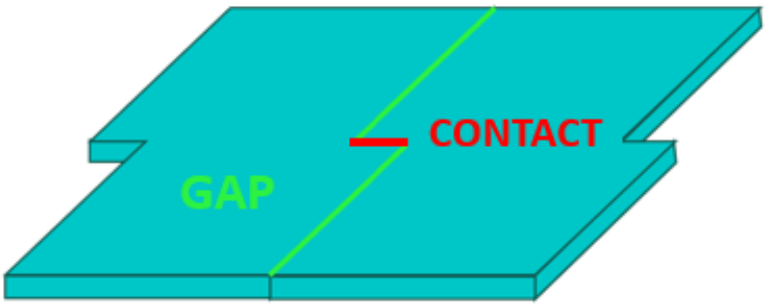

Figure 11: Dummy Shroud Model

The object of the study is only a single blade-disk shrouded component because to analyze all the bladed disk it is used the *cyclic symmetry*, which is a reduction method explained in the following paragraphs.

2.1 Modal Analysis

Modal analysis is a computational or experimental process for predicting or measuring modal parameters. Resonant frequency, mode shapes, and damping are all the modal parameters.Practically Modal Analysis analyzes the ways in which a structure can vibrate. The eigenvalue problem is as follows:

$$([K] - \omega^2[M])\{\Phi\} = 0. \tag{6}$$

Where ω^2 are the eigenvalue, so the frequency and Φ the eigenvectors,the vibration ways. This analysis is done on a not loaded structures.The number of eigenvectors can be decided by the user, because theoretically corresponds to the number of Degrees of Freedom (DOF) of the structure. It is important to understand what type of modes are present:

- **Real Modes**:characterized by the presence of only one eigenvalue, are typical for the bodies with low mechanical coupling in the row.In this case the model can be simplified, removing the disk and fixing the blade at the root (blade-only analysis). If the mode is real all the points of the blade vibrates in phase or in counter phase.
- **Complex Modes**: characterized by the presence of a complex eigenvalue which is made up by the combination of two real eigenvalues in quadrature. There's a high mechanical coupling between blade and disk, this one participates very strongly to the vibration. Here the mode shape is characterized by a wave which passes through the row. According to that, if the mode is complex, there will be some points whit zero shift. A line which unites two of those points is called *nodal*

diameter.

Nodal diameters can best be described by visualizing a flat round plate. If we were to suspend the plate in air, by a string, and tap it sharply with a hammer, we would excite all of modes of vibration[24]. Practically, a nodal diameter is the diameter with displacement zero.

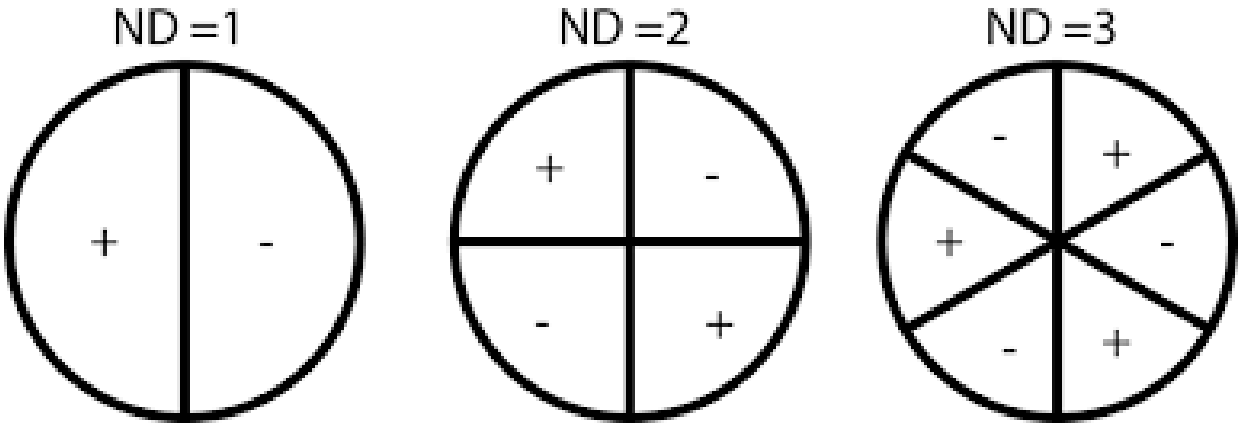

Figure 12: Nodal Diameter example

2.2 Cyclic Symmetry

Cyclic symmetry allows you to analyze a model with circular patterns around an axis by modeling a representative segment. The segment can be a part or an assembly. The geometry, restraints, and loading conditions must be similar for all other segments (cyclically patterned) making up the model.

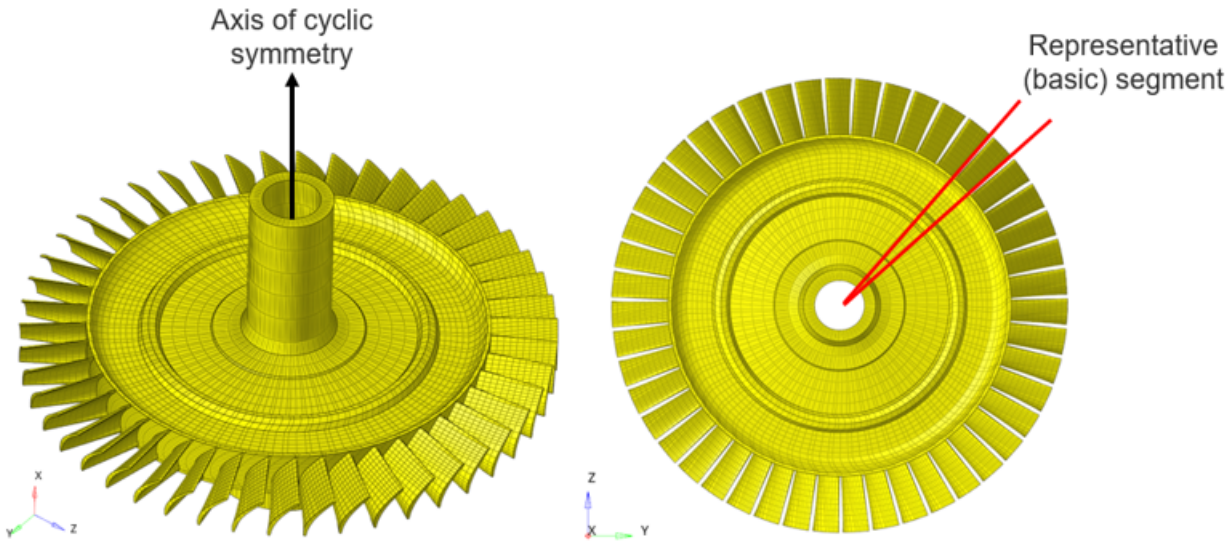

Figure 13: Turbine Sector

In this case each sector is considered equal as the others, it is a tuned systems.Considering the adiacent sectors it is possible to built the complete 360°model simply replicating the model of the single sector N times and coupling the adjacent sectors together.

At the basis of cyclic symmetry modeling is the observation that these components are composed of sectors that are identical to each other (in first approximation) so the analysis of the entire model results superfluous,allowing an easier analysis of the individual sector, as long as the appropriate conditions are applied to outline the problem.

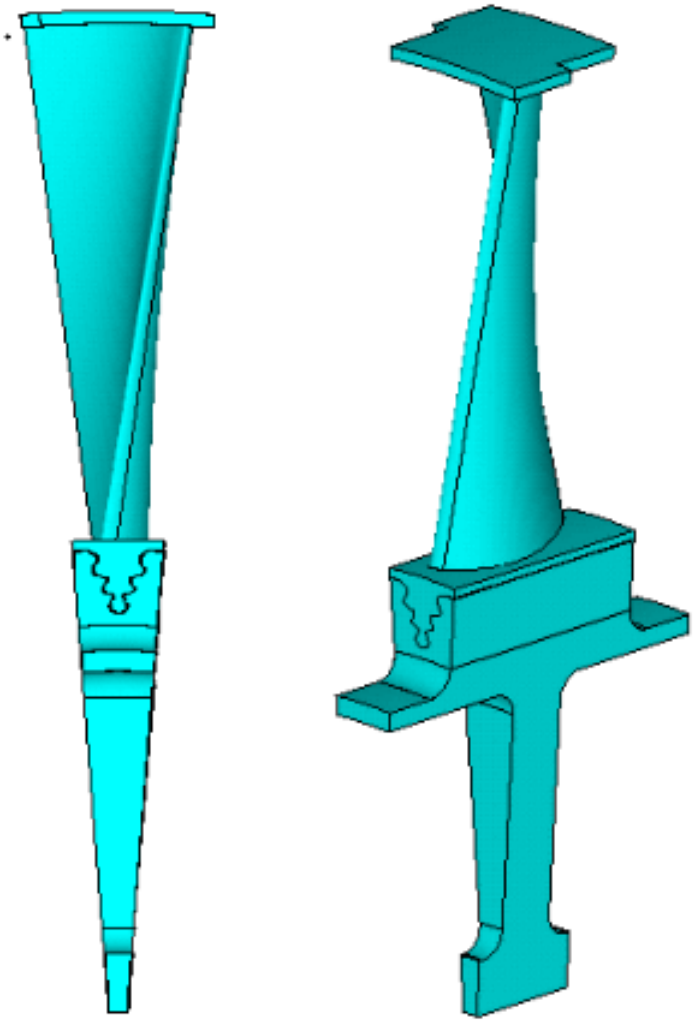

Figure 14: Fundamental Sector

Considering a cylindrical coordinate system, with the z axis coinciding with the rotation axis,it is possible to use the same model for each sector.All this settings and theory are better explained in the picture below:

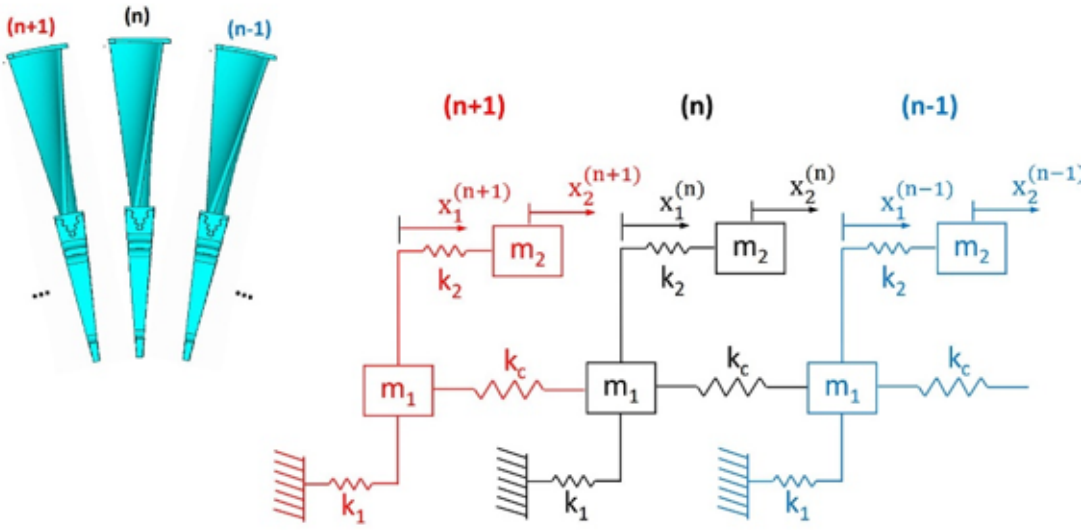

Figure 15: 2D Turbine Sector Model-Cantilever Configuration

Lagrange's equations are used to obtain the equations of motion of the model which are as many as the degrees of freedom (DOF).

$$m_1 \ddot{x_1}^{(n)} + k_1 x_1^{(n)} + k_2(x_1^n - x_2^{(n)}) + k_c(x_1^{(n)} - x_1^{(n-1)}) = 0 \quad (7)$$

$$m_2 \ddot{x_2}^{(n)} + k_2(x_2^{(n)} - x_1^{(n)}) = 0 \quad (8)$$

In compact matrix form:

$$[m^{(n)}]\left\{\ddot{x^{(n)}}\right\} + [k^{(n)}]\left\{x^{(n)}\right\} + [k_c^n]\left\{x^{(n+1)}\right\} + [k_c^{(n)}]\left\{x^{(n-1)}\right\} \quad (9)$$

This is the equation for the generic sector n,it is possible to write the same equation for each sector from 1 to N.In general:

$$[M]\{\ddot{X}\} + [K]\{X\} = 0 \tag{10}$$

The previous model is for a bladed disk with cantilever blade configuration. For this thesis work it's more appropriate to consider a model with a shrouded blade, the scheme became as the picture below:

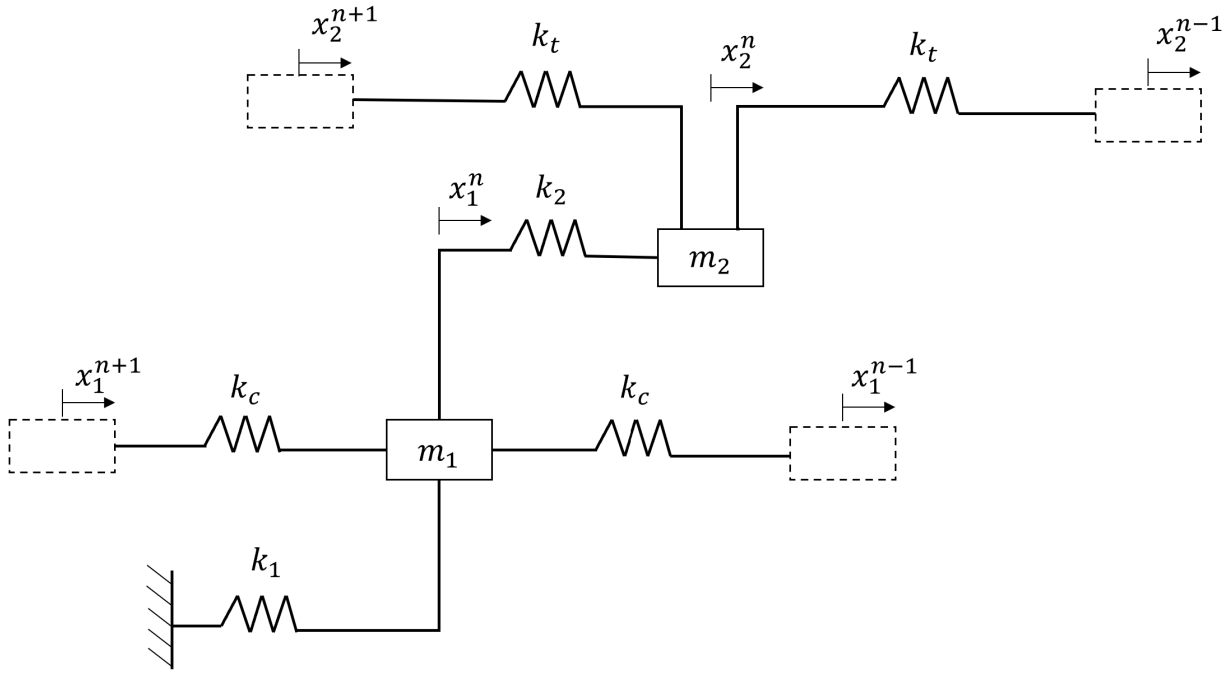

Figure 16: 2D Model for bladed disk with shrouded blade

$$m_1 \ddot{x_1}^{(n)} + k_1 x_1^{(n)} + k_2(x_1^n - x_2^{(n)}) + k_c(x_1^{(n)} - x_1^{(n-1)}) + k_c(x_1^{(n)} - x_1^{(n+1)}) = 0 \tag{11}$$

$$m_2 \ddot{x_2}^{(n)} + k_2(x_2^{(n)} - x_1^{(n)}) + k_c t(x_2^{(n)} - x_2^{(n-1)}) + k_t(x_2^{(n)} - x_2^{(n+1)}) = 0 \tag{12}$$

Compared to the previous configuration, the elastic coupling was added to the tip at the interlock, represented by the stiffness k_t.

Considering a generic mode Φ:

$$\{\Phi\} = \begin{Bmatrix} \Phi^1 \\ \Phi^2 \\ \cdots \\ \Phi^n \\ \cdots \\ \Phi^{N-1} \\ \Phi^N \end{Bmatrix}$$

Body with cyclic symmetry have particular modal properties.There are two type of modes:

- Modes associated with a single eigenvalue:
  They can be:

  1. Equal mode shapes in every sector:

$$\Phi^{(n)} = \Phi^{(n+1)} \tag{13}$$

  2. Equal mode shapes with opposite signin every sector:

$$\Phi^{(n)} = -\Phi^{(n+1)} \tag{14}$$

- pairs of modes with the same eigenvalue.

The pairs of modes with the same eigenvalue are coupled and each couple is associated to a single eigenvalue, so a single value of natural frequency. For the following discussion the following nomenclature will be used: the two eigenvector with the same eigenvalue are called $\{\Phi\}$ and $\{\Phi'\}$.

This two eigenvectors in general are not orthogonal, it is possible to write $\{\Phi'\}$ in this way as a eigenvector:

$$\{\Phi'\} = c\{\Phi\} + s\{\hat{\Phi}\} \tag{15}$$

It is possible to demonstrate that $\{\hat{\Phi}\}$ is orthogonal to $\{\Phi\}$, in addition, if two eigenvectors are orthogonal, normalized and associated to the same eigenvalue, the linear combination of them is an eigenvector. It is possible to declare that:

$$\{\Phi'\} = c\{\Phi\} + s\{\hat{\Phi}\} \tag{16}$$

is an eigenvector.

Moving on, let's consider a complex mode $\{\overline{\Psi}\} = \{\Phi\} + i\{\hat{\Phi}\}$. It is useful

to understand if it is possible to perform a modal analysis for a single sector and then expand the result to the entire disk.

$$\{\overline{\Psi}\} = \begin{Bmatrix} \overline{\Psi}^1 \\ \overline{\Psi}^2 \\ \cdots \\ \overline{\Psi}^n \\ \cdots \\ \overline{\Psi}^{N-1} \\ \overline{\Psi}^N \end{Bmatrix}$$

Imagining to perform a rigid rotation of an angle ϕ equal to the width of the sector, we obtain:

$$\{\overline{\Psi'}\} = \{\Phi'\} + i\{\hat{\Phi}'\} \tag{17}$$

This mode is still a modal shape of the system.It is possible to write the relation between the two mode:

$$\{\overline{\Psi}\} = \{\overline{\Psi'}\}e^{-i\phi} \tag{18}$$

Inserting complex modes is therefore necessary for bladed disks.

Considering the real modes, all the degrees of freedom of the system tend to vibrate in phase with each other, which means that they simultaneously reach the maximum, minimum and null amplitude.

For complex modes this does not happen, between two adjacent sectors A and B, the point of sector A will vibrate with a phase shift ϕ compared to the point of sector B.The dynamics described by the complex mode is therefore a rotating wave with phase shift ϕ between adjacent sectors.To understand the admissible angle ϕ,we do the following discussion:

Considering a bladed disk made up of N sectors, after N rotations we expect to obtain the same eigenvector as the first sector, therefore we must obtain an angle equal to an integer multiple of 360°[5].

$$N\phi = 2\pi h \rightarrow \phi = \frac{2\pi h}{N} \tag{19}$$

where:

- ϕ is the *inter-blade phase angle*;
- h is the *harmonic index* and it is an integer.

Considering:

$$\{\overline{\Psi}^{(n)}\} = \{\overline{\Psi}^{(n-1)}\}e^{i\phi} \rightarrow \{\overline{\Psi}^{(n)}\} = \{\overline{\Psi}^{(n-1)}\}e^{ih\frac{2\pi}{N}} \tag{20}$$

- $\phi = 0 \rightarrow h = 0$: Equal mode shapes in each sector:

$$\overline{\Psi}^{(n)} = \overline{\Psi}^{(n-1)} \tag{21}$$

- $\phi = \pi \rightarrow h = \frac{N}{2}$: Equal mode shapes with opposite sign:

$$\overline{\Psi}^{(n)} = -\overline{\Psi}^{(n-1)} \tag{22}$$

  This mode exist only for even number of sectors N.

- for all the others values of ϕ and h, the modes are all complex, given the periodicity it is possible to consider only the harmonic indicies.
  - h=0,1,2,...,$\frac{N}{2}$-1,$\frac{N}{2}$ if the bladed disk has a even number of sectors;
  - h=0,1,2,...,$\frac{N-1}{2}$-1,$\frac{N-1}{2}$ if the bladed disk has a odd number of sector.

The harmonic index indicates also the number of nodal diameters.

Therefore exploiting the properties of cyclic symmetry and harmonic indices it is possible to perform a modal analysis for a single sector and then expand the solution for all the disk.

2.3 Modal Analysis with cyclic symmetry

Looking at equation (11) and (12):

$$m_1 \ddot{x_1}^{(n)} + k_1 x_1^{(n)} + k_2(x_1^n - x_2^{(n)}) + k_c(x_1^{(n)} - x_1^{(n-1)}) + k_c(x_1^{(n)} - x_1^{(n+1)}) = 0 \tag{23}$$

$$m_2 \ddot{x_2}^{(n)} + k_2(x_2^{(n)} - x_1^{(n)}) + k_c t(x_2^{(n)} - x_2^{(n-1)}) + k_t(x_2^{(n)} - x_2^{(n+1)}) = 0 \tag{24}$$

As written before, there is the hypothesis of harmonic vibrations:

$$\{x^{(n)}\} = \{\overline{x}^{(n)}\}e^{-i\omega t} \tag{25}$$

so:

$$-\omega^2 m_1 \overline{x_1}^{(n)} + k_1 \overline{x_1}^{(n)} + k_2(\overline{x_1}^{(n)} - \overline{x_2}^{(n)}) + k_c(\overline{x_1}^{(n)} - \overline{x_1}^{(n+1)}) + k_c(\overline{x_1}^{(n)} - \overline{x_1}^{(n-1)}) = 0 \tag{26}$$

$$-\omega^2 m_2 \overline{x_2}^{(n)} + k_2(\overline{x_2}^{(n)} - \overline{x_1}^{(n)}) + k_t(\overline{x_2}^{(n)} - \overline{x_2}^{(n-1)}) + k_t(\overline{x_2}^{(n)} - \overline{x_2}^{(n+1)}) = 0 \tag{27}$$

Considering the relation of the cyclic symmetry:

$$\{\overline{\Psi}^{(n)}\} = \{\overline{\Psi}^{(n-1)}\}e^{ih\frac{2\pi}{N}} \tag{28}$$

$$\overline{x_1}^{(n)} = \overline{x_1}^{(n-1)}e^{-ih\frac{2\pi}{N}} \rightarrow \overline{x_1}^{(n-1)} = \overline{x_1}^{(n)}e^{-ih\frac{2\pi}{N}} \tag{29}$$

$$\overline{x_1}^{(n+1)} = \overline{x_1}^{(n)}e^{-ih\frac{2\pi}{N}} \tag{30}$$

The equations of motions become:

$$-\omega^2 m_1 \overline{x_1}^{(n)} + k_1 \overline{x_1}^{(n)} + k_2(\overline{x_1}^{(n)} - \overline{x_2}^{(n)}) + k_c(\overline{x_1}^{(n)} - \overline{x_1}^{(n)e^{-ih\frac{2\pi}{N}}}) + k_c(\overline{x_1}^{(n)} - \overline{x_1}^{(n)}e^{-ih\frac{2\pi}{N}}) = 0 \tag{31}$$

$$-\omega^2 m_2 \overline{x_2}^{(n)} + k_2(\overline{x_2}^{(n)} - \overline{x_1}^{(n)}) + k_t(\overline{x_2}^{(n)} - \overline{x_2}^{(n)} e^{ih\frac{2\pi}{N}}) + k_c(\overline{x_2}^{(n)} - \overline{x_2}^{(n)} e^{-ih\frac{2\pi}{N}}) = 0 \quad (32)$$

In matrix form:

$$\left(-\omega^2 \begin{bmatrix} m_1 & 0 \\ 0 & m_2 \end{bmatrix} + \begin{bmatrix} k_1 + k_2 + 2k_c - k_c e^{ih\frac{2\pi}{N}} - k_c e^{-ih\frac{2\pi}{N}} & -k_2 \\ -k_2 & k_2 + 2k_t - k_t e^{ih\frac{2\pi}{N}} - k_c e^{-ih\frac{2\pi}{N}} \end{bmatrix}\right) \begin{Bmatrix} \overline{x_1}^{(n)} \\ \overline{x_2^{(n)}} \end{Bmatrix} = \begin{Bmatrix} 0 \\ 0 \end{Bmatrix} \quad (33)$$

From the outputs of the modal analysis it can be plotted the freND diagram(**freND→fre**quency vs **N**odal **D**iameter). In the x-axis there are the Nodal Diameter , instead in the y-axis there are the frequencies. This diagram describes how the value of the natural frequency of a mode shape changes respect the Nodal Diameter.

This graph makes us notice that as the nodal diameter increases the natural frequency increases, the aforementioned growth tends to fall to zero so that for high nodal diameters the frequency maintains more or less the same value tending towards an asymptotic value.

The reason why this happens is quite intuitive, for high nodal diameters the structure is more rigid, the stiffness increases.

Other salient areas of the diagram may be the veering areas, i.e. when two modal families exchange modal shapes.

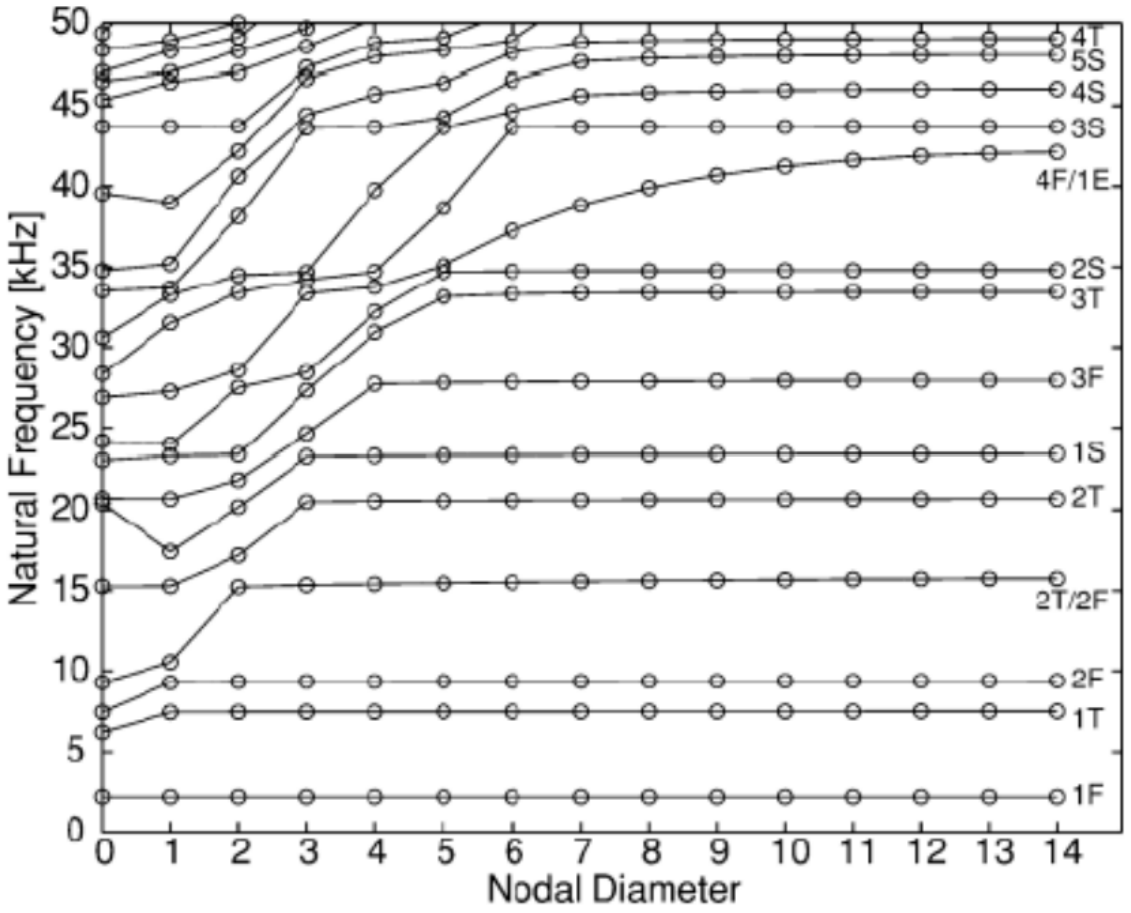

Figure 17: freND Diagram example

2.4 Forced Response

A Forced Response Analysis is useful to identify and verify the presence of resonances within the operating range of the machine and the amplitude of the response. A Low Pressure Turbine has various types of loads during its operating life. The most important are:

- Pressure Loads:the turbine must rotate to drive the compressor, this rotational movement is given by the different pressure between suction side and pressure side of LPT;
- Thermal Loads: the turbine must be in contact with the hot gases

come from the combustor to cool them, so it is subject to thermal gradients.

- Inertial Loads: the turbine has an high angular velocity that generate centrifugal forces;
- Pre-Twist Loads: all the blades are subject to a pre-load when they are installed,the pre-load is useful to obtain the correct positioning of the airfoil with respect to the flux in the operating life.

There are two families of vibrations, synchronous or non synchronous:

- to the first family belongs the force response where the source is an unsteady pressure field which induces vibrations whose frequency is a multiple of the angular velocity;
- to the second flutter and other NSV where the sources can be multiples: rotor stall or flux instability, which induce vibrations whose frequency are not related to the angular velocity of the turbine.

In the Campbell's Diagram are exposed all the vibrations, in the x-axis there is the shaft speed in RPM, in the y-axis there is the frequency in Hz, from this diagram is possible to see the hypothetical resonance zones [5].

The dynamic loads that cause synchronous vibrations (so Forced Response) can be described by using the Fourier series as function of the angle $\alpha = \Omega t$:

$$F(\alpha) = F_0 + \sum_{EO} F^{(EO)} cos(EO\alpha + \delta) \tag{34}$$

The generic component EO of the harmonic force is identified by a parameter called *Engine Order*, which is defined as:

$$EO = \frac{\omega}{\Omega} \tag{35}$$

So it can be written as:

$$F^{(n)} = F^{(EO)} cos(\omega t + \delta) \tag{36}$$

The study of the forced response consists in understanding if exciting loads can represent dangerous conditions for the turbine. These conditions are resonance condition and it happen when the frequency of the exciting load coincides with one of the natural frequencies of the system.

The cross zone are called "hypothetical" resonance zones because crossing is a necessary condition but not sufficient for resonance.Focusing on a crossing, there is the harmonic index h that is related to the natural frequency if the system, the crossing is a resonance condition only if:

$$h = EO$$

The harmonic index value must be equal to the Engine Order to represent a resonance condition.

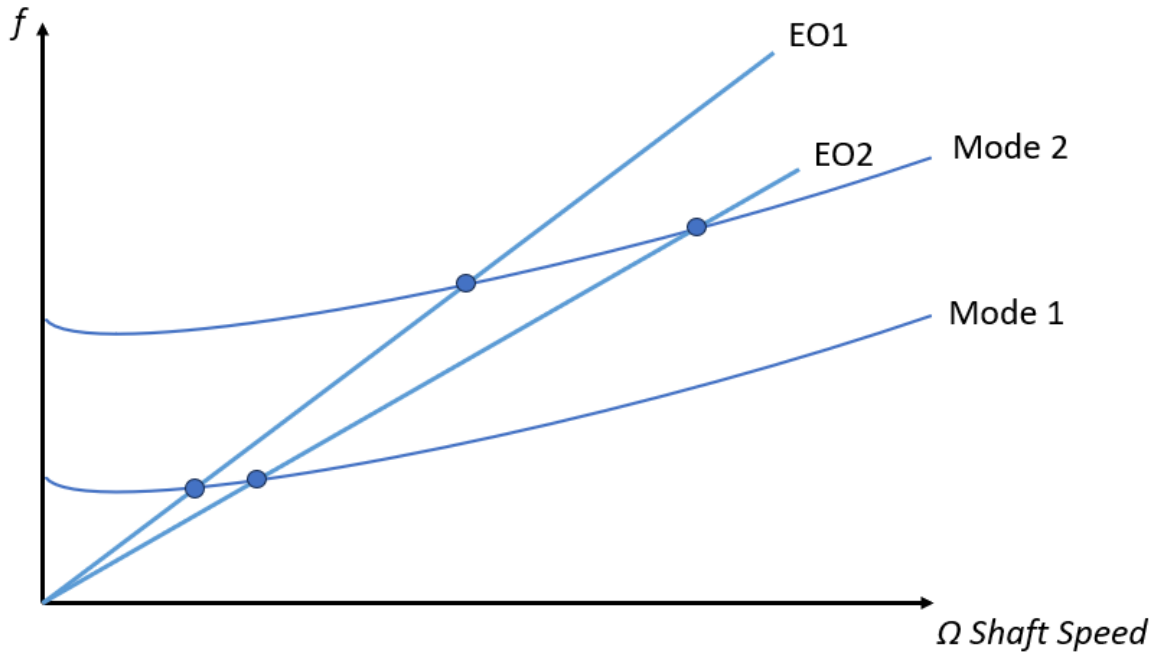

Figure 18: Campbell's Diagram

As written before, the harmonic index h can assume the following values:

$$0 \leq h \leq N - 1$$

EO values can be greater than N-1. It can be demonstrated that for:

$$EO \geq N - 1$$

The resonance condition is represented by:

$$EO - kN = h \tag{37}$$

where k = 0, 1, 2, 3, ..., depending on the value of the EO. To understand which value of h and EO can causes resonance, it is used the *Zig Zag Diagram*. This diagram is characterized by harmonic index h on x-axis and EO in y-axis.

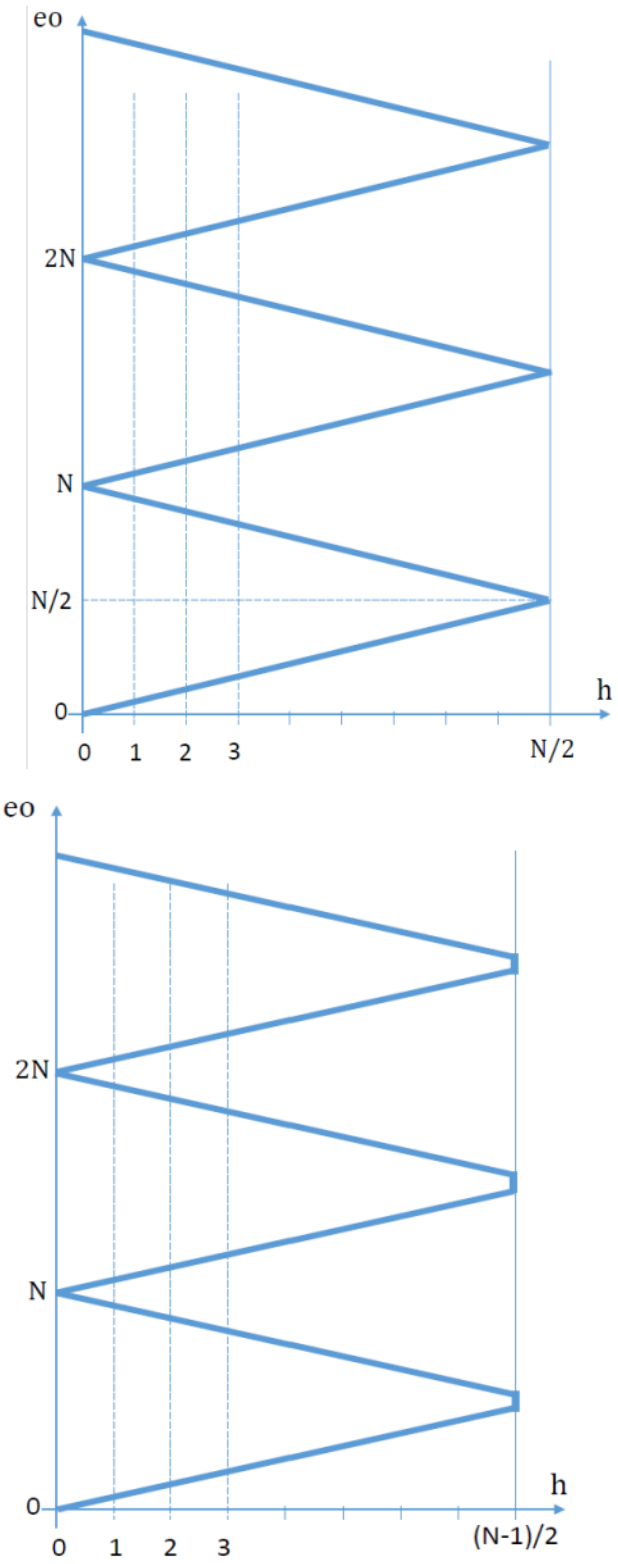

Figure 19: Types of Zig Zag Diagram

2.5 MAC: Modal Assurance Criterion

The MAC is a statistical indicator , just like the ordinary coherence. It is a number useful to compare the results obtained from two different modal analysis. These difference could come from the model, technique of solution or if it's used a reduction method. The MAC was originally introduced in modal testing as an additional confidence factor in the evaluation of modal vector from different excitation locations.

The MAC number is a scalar between 0 and 1, a MAC value higher than 0.9 is a synonymous of a good match between the vectors.

The MAC is calculated as a normalized scalar product of two vectors, $\{\phi_X\}$ and$\{\phi_A\}$ and the results are arranged into the MAC matrix:

$$MAC(r,q) = \frac{|\{\phi_A\}_r^T\{\phi_X\}_q|^2}{(\{\phi_A\}_r^T\{\phi_A\}_r)(\{\phi_X\}_r^T\{\phi_X\}_q)} \tag{38}$$

Where $\{\phi_X\}_q$ is the test modal vector, mode q, $\{\phi_A\}_r$ is the compatyble modal vector, mode r and the apex T stands for the operation of transposition.

For complex mode the expression became:

$$MAC(r,q) = \frac{|\{\psi_A\}_r^T\{\psi_X\}_q'|^2}{(\{\psi_A\}_r^T\{\psi_A\}_r')(\{\psi_X\}_r^T\{\psi_X\}_q')} \tag{39}$$

Where $\psi^{'}$ is the complex coniugate of the vectors.

To visualize the MAC magnitude it is used a color plot 2D or 3D. It is important to underline that MAC is only a discrete calculation and a coherence index.[7]

In the picture below there is an example: in the two axis there are the

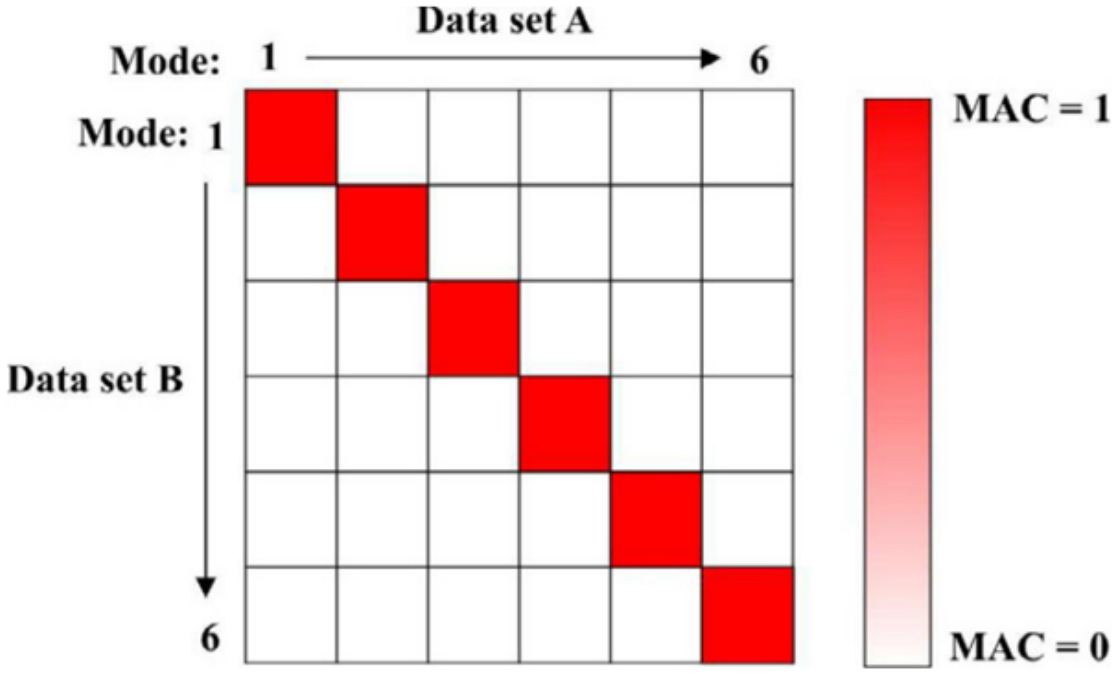

Figure 20: MAC 2D Plot

modes of the two analysis, so we compare mode by mode. In the picture is possible to see that the modes of the two analysis are coherent among them. The MAC is equal to 1, along the diagonal of the matrix so the vector is exactly the same.

3 Aeroelasticity

3.1 Overview

The Aeroelasticity is the discipline that brings together different disciplines and studies their mutual interaction, it is the study of the interactions between the *Inertial* (I), *Elastic* (E) and *Aerodynamic* (A) forces occurring while a non-rigid body interact with a fluid flow. These interactions are described by *Collar's triangle*. The simultaneous interaction

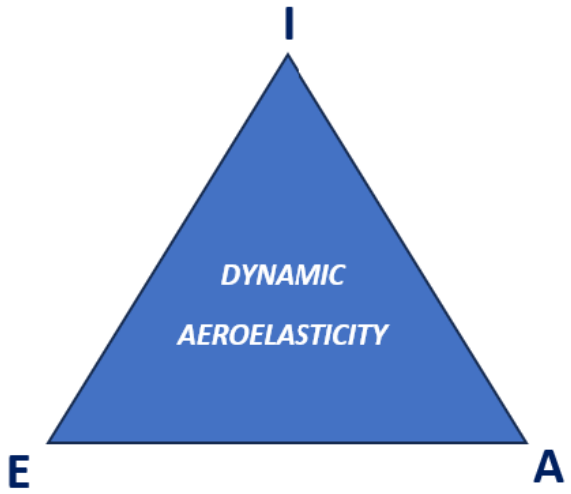

Figure 21: Collar's Triangle

of all three forces gives shape to *Dynamic Aeroelasticity*, which deals with the dynamic response of the body, typically vibrational.
Focusing on the forces, in the following section it is possible to highlight each contributes:

1. The inertia of a body places an important role in the study of aeroelasticity. The **inertia forces** depend on how the masses are positioned and are related to the mass property of the structure.

2. The **elastic forces** are related to the material property, consequently to the system's deformation.

3. The **aerodynamic forces** are the only external forces, their impact comes from the fluid where the body is immersed. They made the airplane able to fly and maneuver.

Each side of the triangle is linked to a discipline, the coexistence of all three is the representation of Dynamic Aeroelasticity. Focusing on each side:

- **E+I**=*Structural Dynamics*, the study of the motion of structures in the most general way excluding rigid motion.

- **A+I**=*Flight Mechanics*,it is considered only the aerodynamic inertia, the aircraft is considered rigid as well as its oscillation.

- **E+A**=*Static Aeroelasticity*,it deals with the static (or steady state) response of an elastic body to a fluid flow.

It is possible to modify Collar's triangle by adding the problem of the commands to obtain the Collar's Pyramid which represents the *Aeroservoelasticity*, this discipline is useful for military designs.

The aim is to understand the interactions between Aerodynamics and Mechanics, in particular the vibrations that can lead to the rupture of the component. Aeromechanics problems are crucial for turbomachines. In a turbomachine there is also the effect of the blades row, the blade is not isolated from the rotor complex, but it suffers from the effect of the other blades.

Aeroelastic issues are more intense as the structure is lighter and more charged. All the aeroelastic problems answer at the following equation:

$$m\ddot{x} + kx = f(t) \tag{40}$$

In the aeronautical field, aeroelastic problems are very frequent, because aeronautical structures are required to be light and resist large aerodynamic loads. Focusing on the aeroelastic problems, the most important are divergence, control reversal and flutter.

- **Divergence**:The angle of attack is increased by aerodynamic forces, thus increasing the torsional stiffness of the wing until it is broken.
- **Control Reversal**: The control activation is no longer effective; the aerodynamic forces configuration brings the control surface to instability until the command is reversed.
- **Flutter**:uncontained vibration that can lead the aircraft to the destruction.

As written in the previous chapter,turbines are subject to various vibration sources, some of which are unreachble under normal operating conditions.

Vibrations induce alternating stresses in the affected elements, if the vibrations are excessive the ultimate stress could destroy the material because the amplitude of the vibrations and σ_n are in scale with each other. If the vibration are moderate , this represent an issue for the fatigue HCF.It is crucial to predict and to prevent vibrations for the turbine design.As we saw, the vibrations can be synchronous or non synchronous, to the first family belongs the force response , to the second flutter and other NSV.

3.2 Flutter

Flutter is a self-excited vibration phenomenon caused by the mutual coupling of the inertial force,elastic force and aerodynamic pressure when the structure is exposed to airflow. When the flight speed is increased to a certain critical value, the vibration remains unchanged, this velocity is called the critical flutter speed.

The most critical part of a jet engines, as just said before, under the aeroelastic point of view, are the slender blades with a high aspect ratio: fan blades and LPT blades. These components, which are very sensible to vibrations, could go on flutter if the fluid in some situation supplies too much aerodynamic work on them. Flutter so, is the principal source of NSV in LPTs.

Flutter phenomena is different between wings plane and turbomachines blades, in the first the instability is created by specific speed of flight and specific aerodynamics conditions, in the second the instability is given by the existence of the other blades, the blades therefore influence each other.

Flutter is such a dangerous phenomenon, if a blade goes into flutter it could easly propagate to the others blades and destroys the entire row.[23]

The study of flutter increased after the collapse of the Tacoma Narrows Bridge in 1940. The wind excited the Torsional modeshape of the bridge putting it in flutter, the phenomenon was destructive and the bridge fallen. After this catastrophe, in the years many methods were developed, some methods were based on panel's theory where it was done a tentative to couple FEM results and Aerodynamic Loads. These methods were quite

Figure 22: Tacoma Narrow Bridge after flutter phenomenon [20]

accurate.

Today the state of the art of aeroelastic analysis consists in a 3D detailed CFD analysis associated to a structural modal analyisis, in the way to perfectly study the fluid structure interaction.

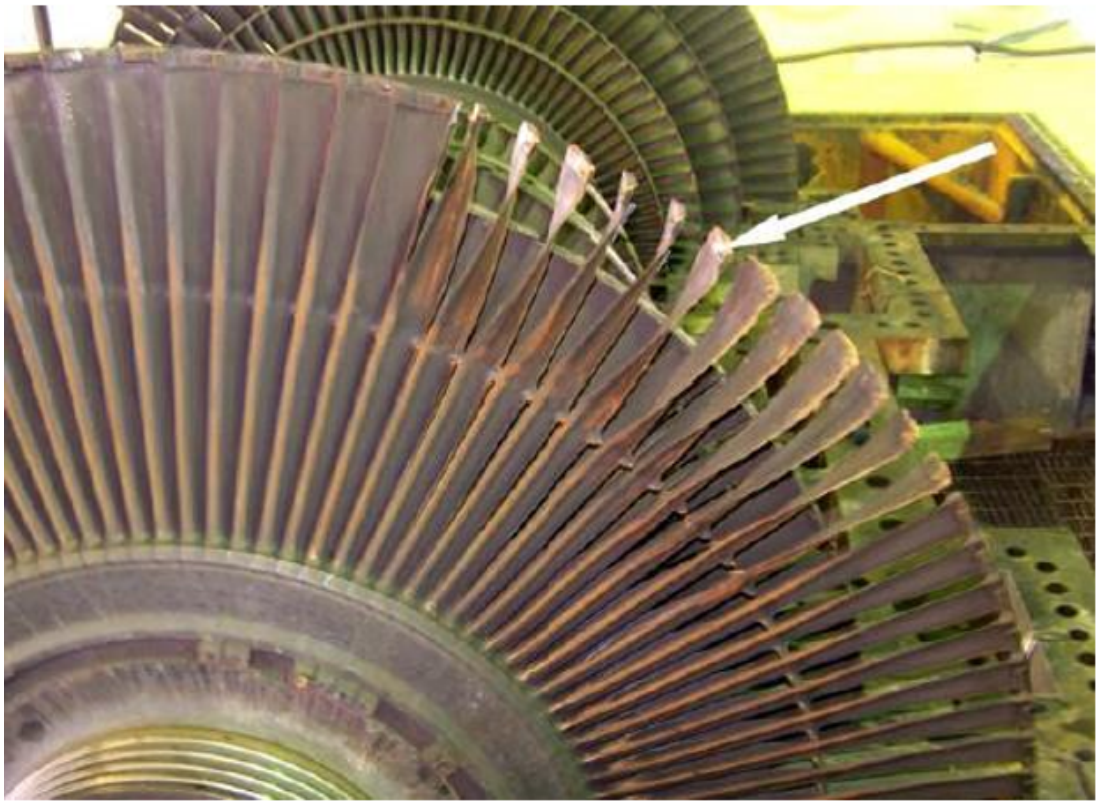

Figure 23: Flutter damage in a LPT [8]

There are various types of flutters that can occur in turbomachines:

- **Classical Flutter**: is the flutter caused by the phase leg between the vibration of the blade and the aerodynamics forces. Is the most common flutter and it shows up without any separations.
- **Coalescence Flutter**: is the flutter generated by the merging of two natural frequencies.
- **Stall Flutter**:is the flutter caused by the stall condition.
- **Dynamic Stall Flutter**:is the particular condition when the bladerow is in stall condition only in a part of the vibration cycle.
- **Choke Flutter**: is the flutter caused by choke condition.

- **Supersonic Unstalled Flutter**: is a type of flutter that shows up when the flow becames supersonic.

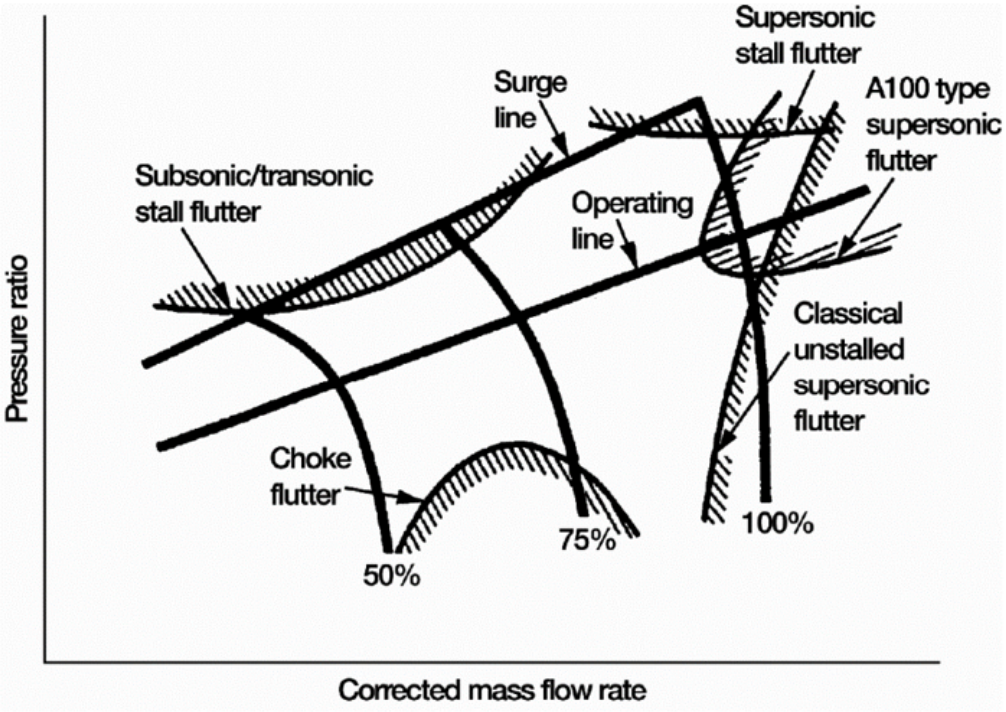

Figure 24: Classification of Flutter type

For free vibrations it is expected the conservation of energy.

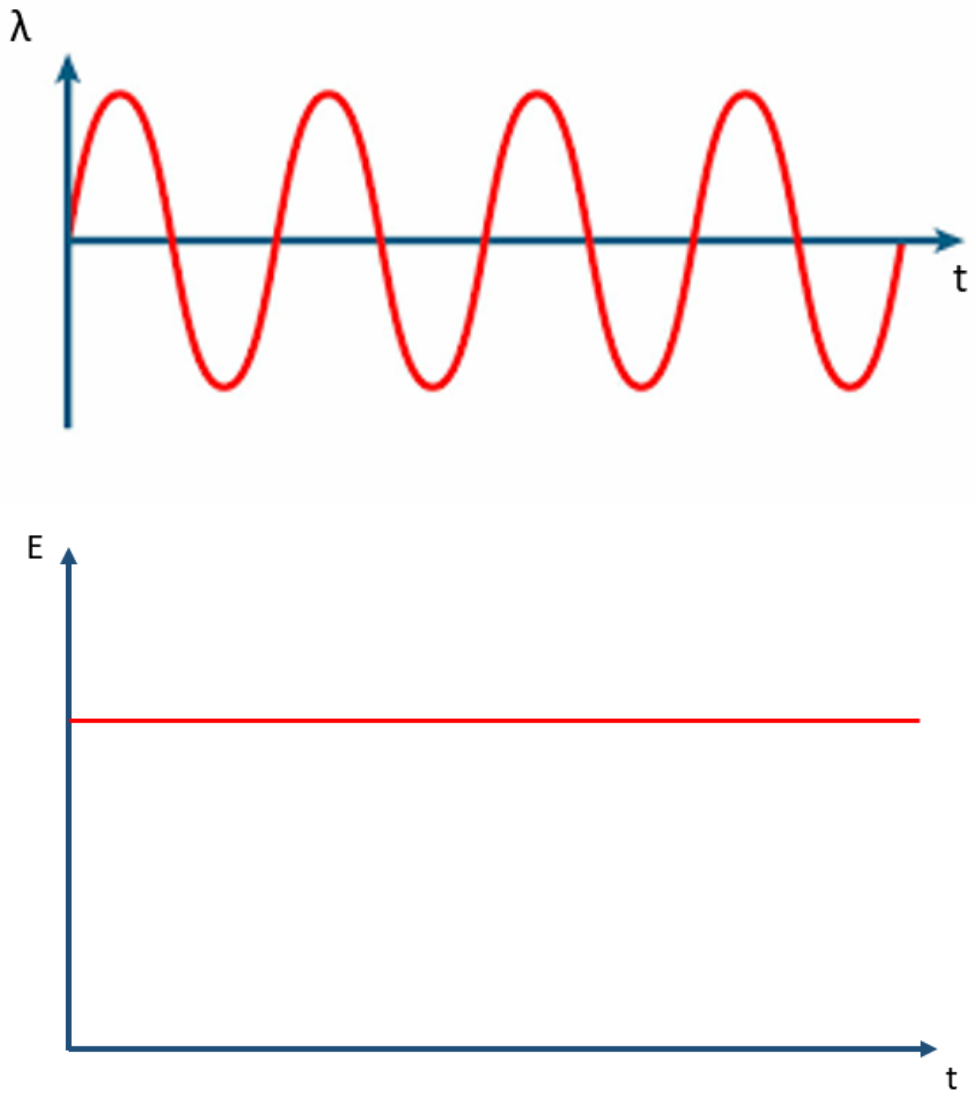

Figure 25: Free Vibration Energy

Severe phenomena induce the energy dissipation causing the decreasing of the amplitude.

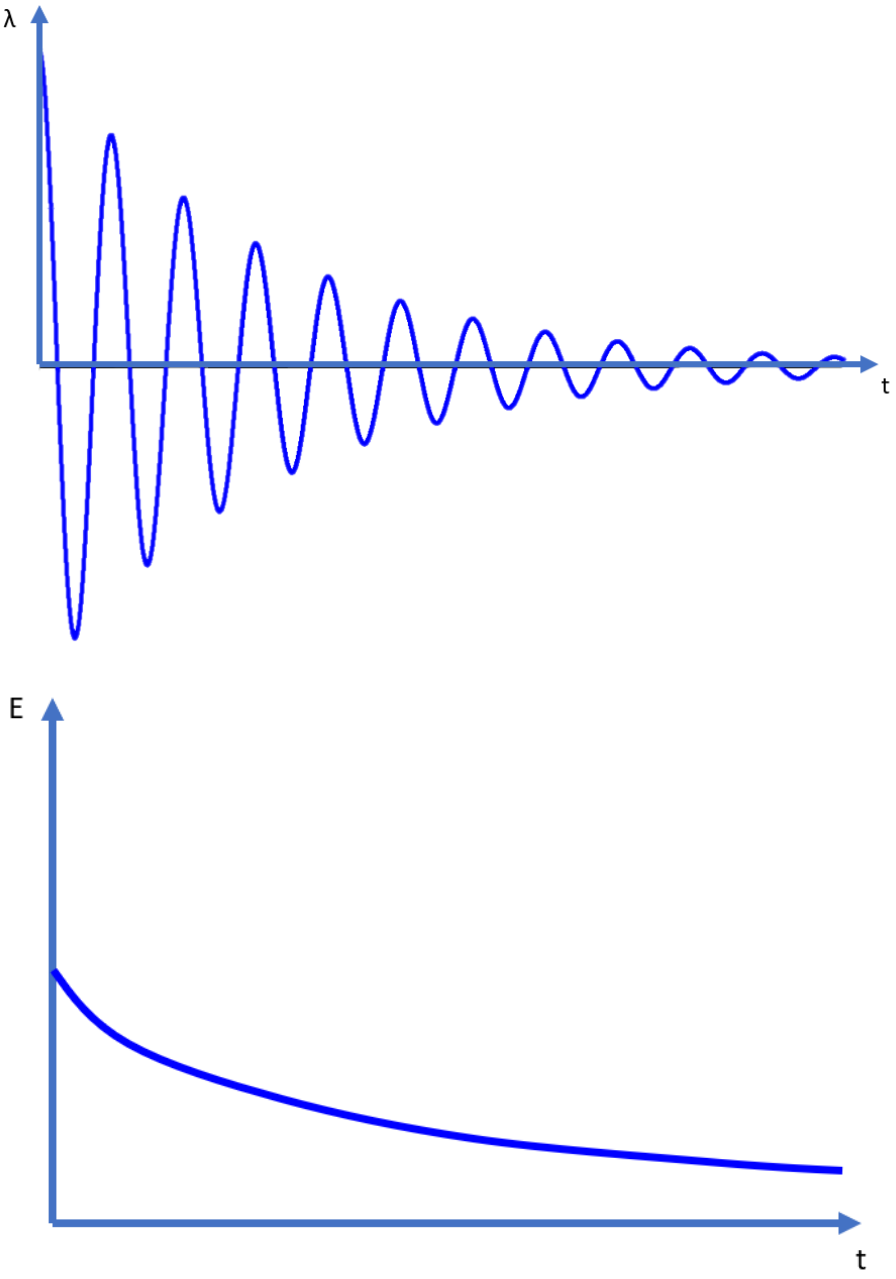

Figure 26: Dumped Energy

There are phenomena that can increase the amplitude by stealing work from the flow to increase the mechanical energy, one of this phenomena is flutter.

4 Flutter Stability

To understand the flutter stability it is necessary to introduce the *reduced velocity*:

$$V_{red} = \frac{V}{\omega b} \tag{41}$$

V is the flow velocity and ω is the frequency of the vibration of the blade and b is the semi-chord of the profile.
This parameter stabilizes itself if decreases.

It is also used the reciprocal of the V_{red}, which is called *reduced oscillatory frequency*:

$$k = \frac{\omega b}{V} \tag{42}$$

In this case obviously increasing k is stabilizing. In the following paragraphs it will explained the concept of *aerodamping* and how this is linked to the stability.

4.1 Flutter Analysis

Flutter methods are aimed at assessing the self-induced pressure response of the fluid flow due to a vibrating component, and how this unsteady pressure can self-sustain the vibrations. To perform a Flutter Analysis there are some Numerical Unsteady Methods. All this methods can be:

- **Coupled Method**:This type of method solves the CFD Steady State and the FEM Analysis simultaneously , is the most precise method but it is very complex and it takes high computational cost.

- **Uncoupled Method**:The CFD Steady State Analysis and the FEM Analysis are solved separated, this method is preferred than the Coupled because is less complex.

The *Uncoupled Method* solves the Structural problem and the Fluid dynamics problem in a separated way.

The *Structural problem* is solved by FEM Analysis that performs a modal analysis to obtain the natural frequencies and the structure's mode shapes.

The *Fluid dynamics problem* is solved in two step:

- Step 1: CFD Steady State to initialize the flow;
- Step 2: CFD Unsteady, in this step are imposed the results of the FEM analysis.

The tool used is the TRAF,which is a finite volumes code developed by University of Florence especially for internal fluxes, which by imposing the FEM results solves the Navier-Stokes to find the Aerodynamic Work:

$$L = \int_t^{t+T} \int (-p) \overline{N} \overline{c}_{blade} d\Sigma dt \tag{43}$$

Then it is calculated the Aerodamping density:

$$\rho\zeta = -\frac{-dL_\delta}{8\pi E_k \frac{d\Sigma}{\Sigma}} \tag{44}$$

The integral of equation (44) is call *Aerodamping*:

$$\zeta = \frac{-L}{8\pi E} \tag{45}$$

Based on the sign of the work for a given nodal diameter it can be established whether this is stable or unstable to flutter:

- If the aerodynamic work is negative (L<0) then the aerodamping will be positive, therefore the structure gives work to the flow.

$$L < 0 \rightarrow \zeta > 0 \rightarrow STABLE$$

- If the aerodynamic work is positive (L>0) then the aerodamping will be negative, therefore the flow gives work to the structure,increasing the vibrations amplitude..

$$L > 0 \rightarrow \zeta < 0 \rightarrow UNSTABLE$$

In the picture below there is an example of Aeroplot, in the y-axis there is the Aerodamping, in the x-axis there are Nodal Diameters:

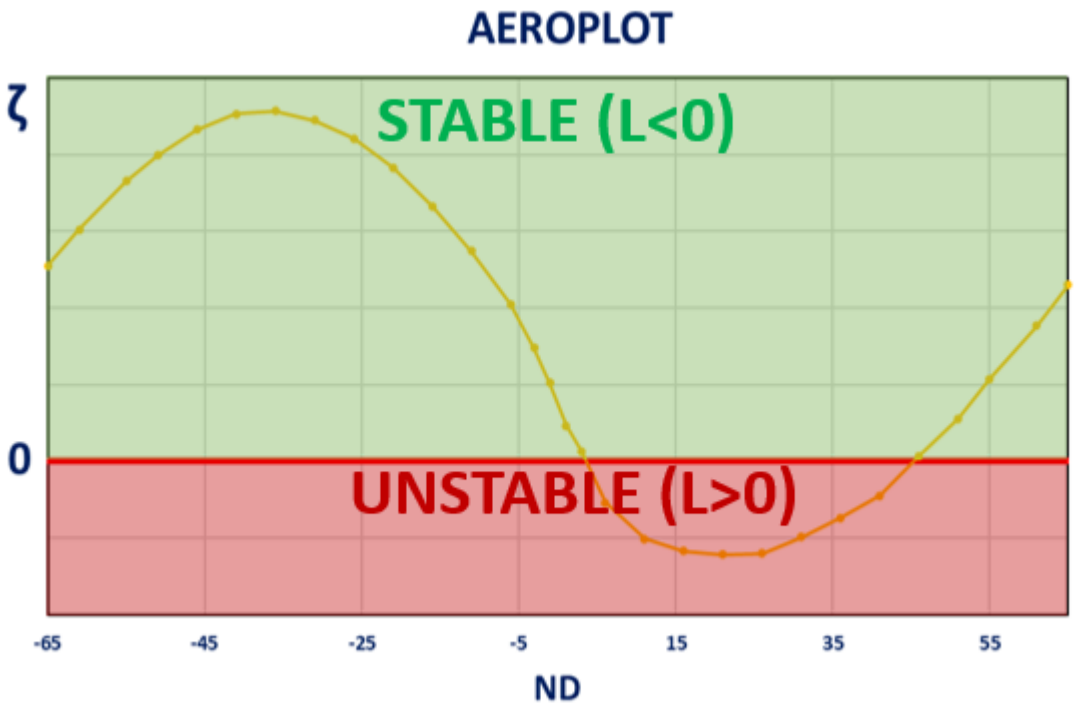

Figure 27: Aerodamping plot example

The graphic is divided in two sections : stable and unstable section. The delimitation f these two sides is x-axis, the zero is the LIMIT of the Flutter Stability.

For this thesis work it is followed an Uncoupled approach.
In the picture below is showed the approach to perform a Flutter Analysis:

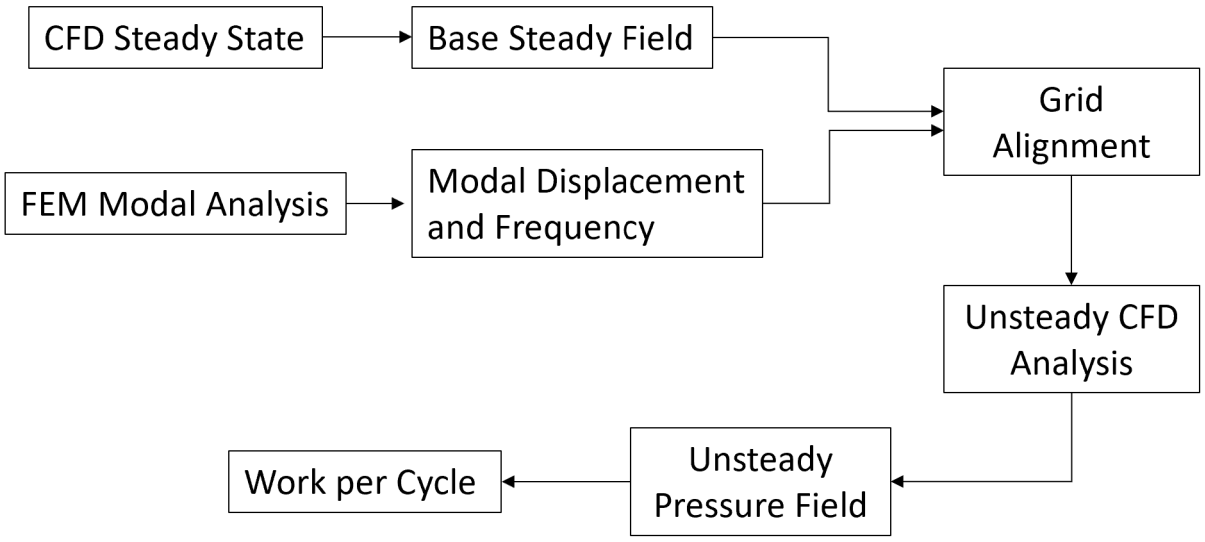

Figure 28: Flutter Analysis Uncoupled Method workflow

5 Flutter 3D Analysis

This section is completely dedicated to the numerical 3D flutter Analysis and its results. There are explained in the detail all the steps to execute the analysis.

5.1 FEM Modal Analysis

The subject of our study as we said before is a LPT bladed disk configuration, this component is a cycle-symmetric solid, so it is possible to perform a Modal Analysis with Cyclic Symmetry.

The blade is a shrouded blade and the fundamental sector blade-disk complex was modeled with Ansys APDL and Hypermesh, but for business privacy reasons the blade will be secreted and a dummy model will be shown in its place.

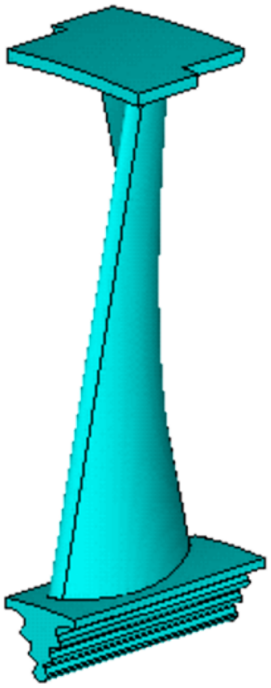

Figure 29: Dummy Model of the Blade

Figure 30: Frontal view of Dummy Model

To perform the analysis were applied the following Boundary Conditions:

- Cyclic Symmetry

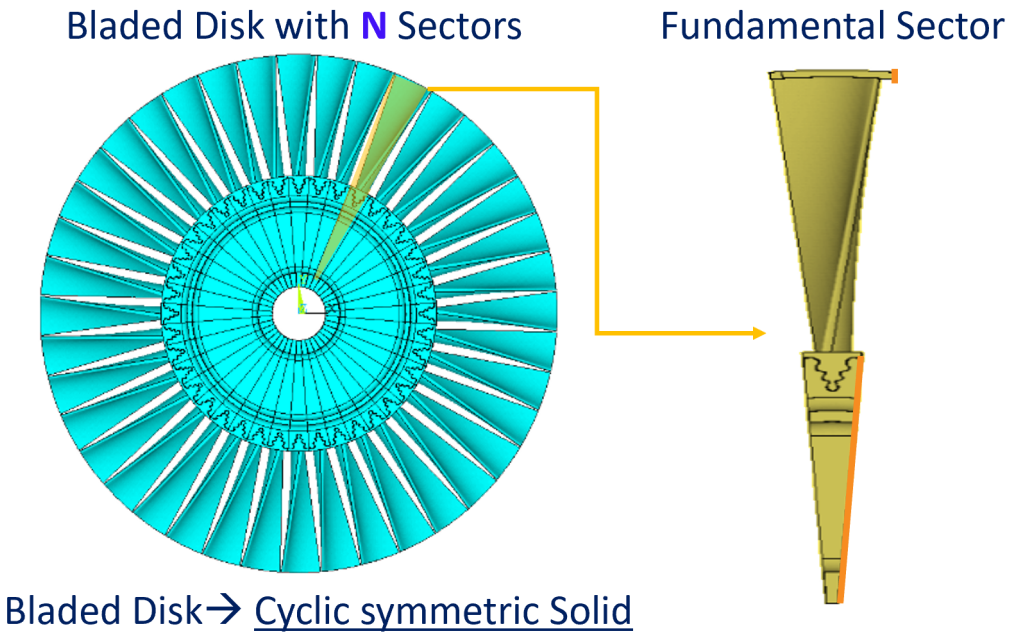

Figure 31: Isolation of the Fundamental Sector

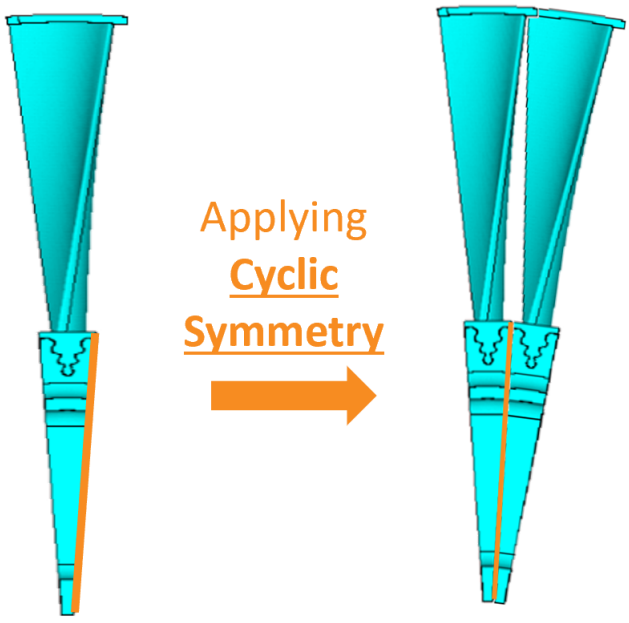

Figure 32: Cyclic Symmetry applied on the model

- Axial and Tangential disk DOFs Locked

  It is absolutely necessary to define the movements prohibited to the disk, in this case the axial and tangential ones.

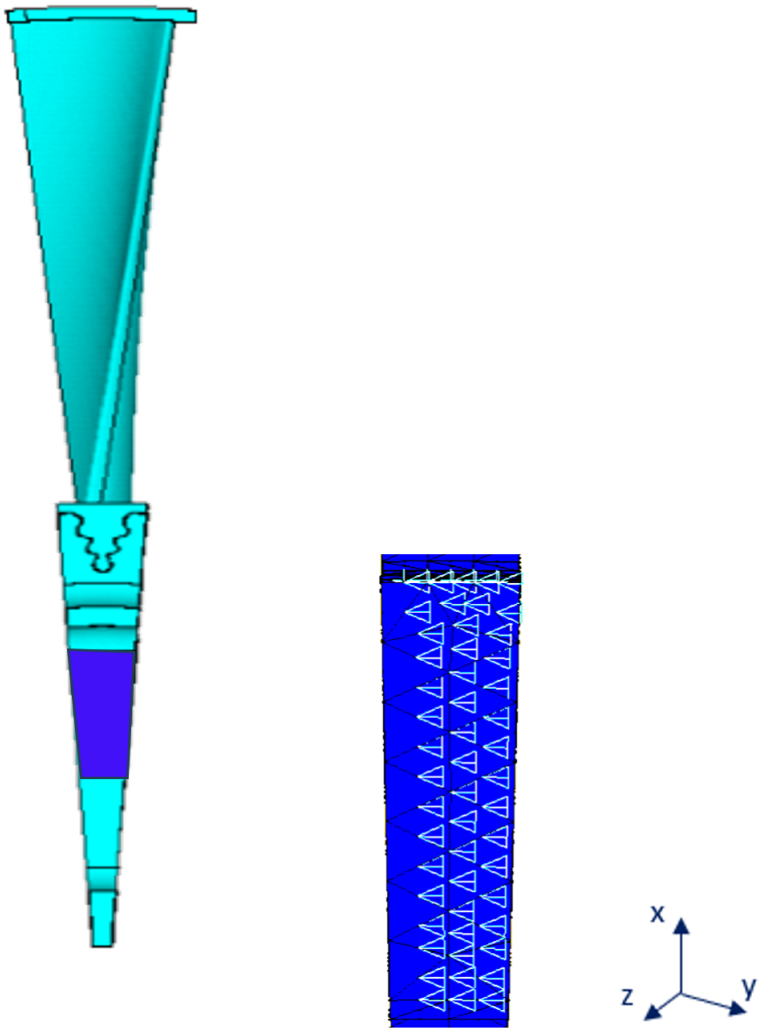

Figure 33: Axial and Tangential disk DOFs constrained

- Blade/Disk Interfaces

  The contact created between the disk and the blade turns out to be another boundary condition, as we want the blade to be keyed to the disk.

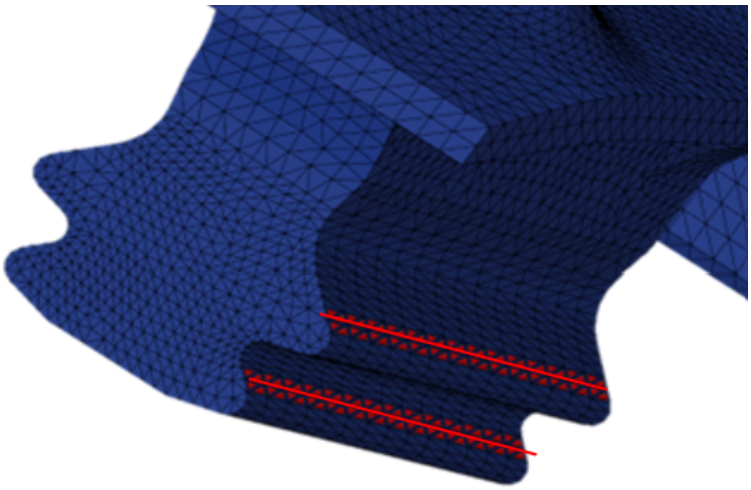

Figure 34: Sets Blade-Disk

- Interlocking Boundary Conditions

  it is necessary to define the type of contact at the interlocking.

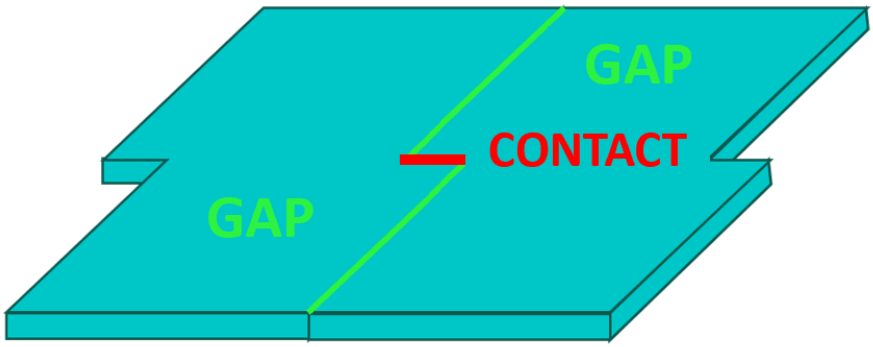

Figure 35: Interlocking Boundary Conditions

The last Boundary Condition is the most significant for this thesis work,

in the next paragraph it will be explained the three cases of study chosen and why.

The Modal Analysis was performed for each case of study to obtain all the modeshapes and to see the impact on flutter stability.

5.1.1 Interlocking Boundary Conditions

As we saw in the Chapter 2, when a shrouded blades i assembled a on the disk it is plausible that there is a contact at the interlock. So the

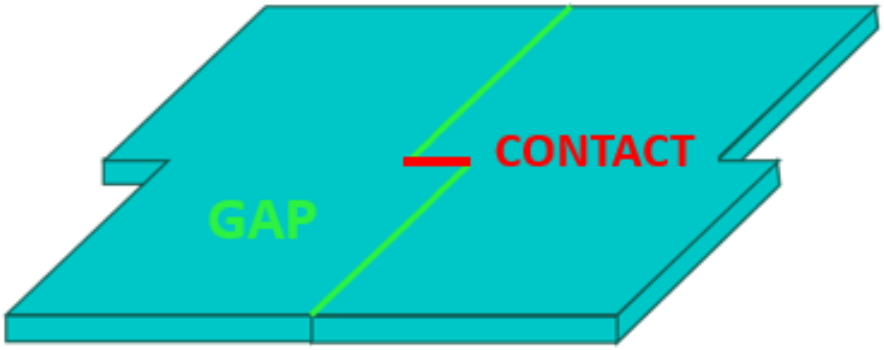

Figure 36: Dummy Shroud Model

idea is that there is a contact, but we don't know what kind of contact can be created, moreover contacts are usually non linear phenomena. The problem to be analyzed is therefore not trivial, to try to simplify it while still obtaining consistent results we choose to work with linear contacts.For the sensitivity of this work are choosen two cases of linear contact:

- Case 1: TIGHT CONTACT
  A total contact is imagined, so all the DOFs of the nodes of the interlocking surface are locked.

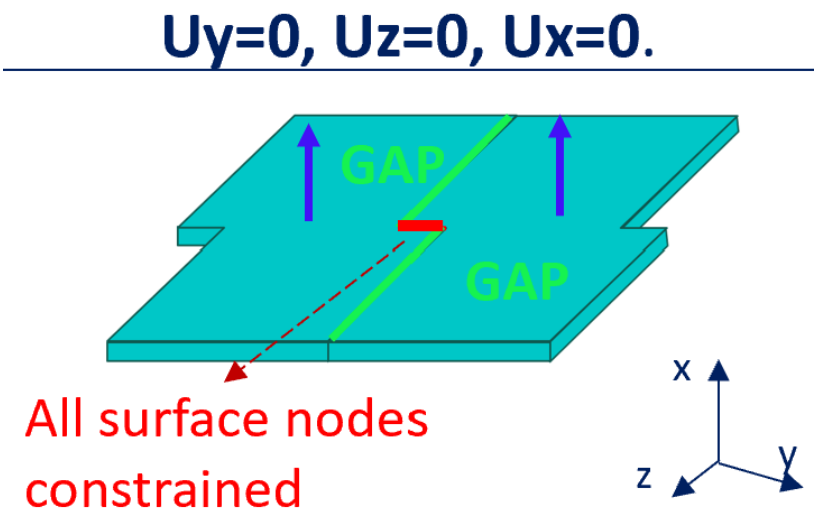

Figure 37: TIGHT CONDITION

- Case 2: RADIAL FREE CONTACT
  Due to a non-optimal assembly, for reasons of tolerance or wear it is imagined that the contact has a degree of free freedom, in this case the radial one.

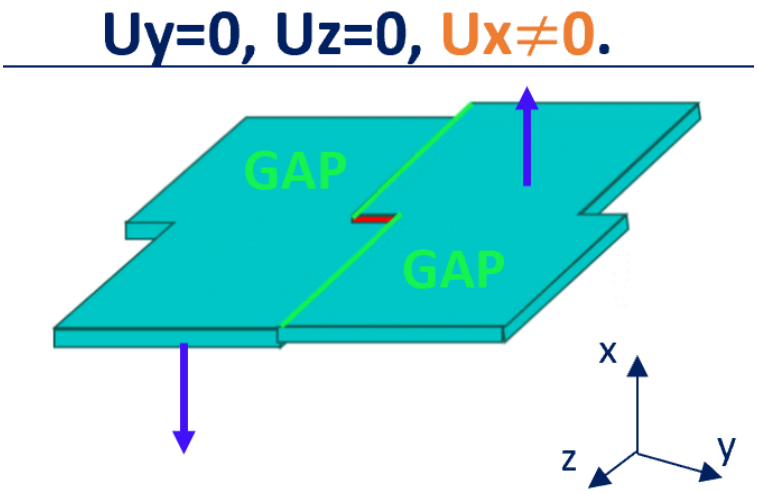

Figure 38: RADIAL FREE CONDITION

A third case, that of non-contact, is also treated. During the service life of the component the contact tends to diminish until it disappears completely, it is therefore interesting to understand what happens if this contact were to vanish.

- Case 3: TIP FREE

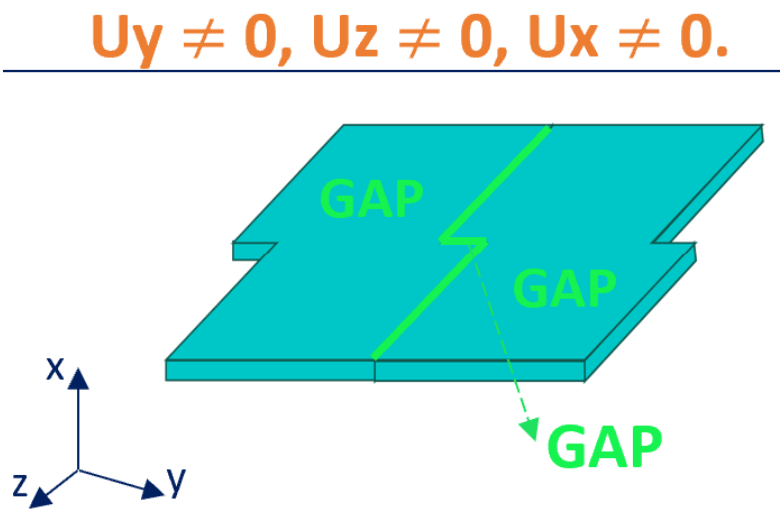

Figure 39: TIP FREE CONDITION

5.1.2 FreND and Modes Shapes Classification

After performing the Modal Analysis for each cases,the results are processed. For this analysis we will be interested in the first two modal families.

For the recognition of the modeshapes are shown the figures of the dummy model:

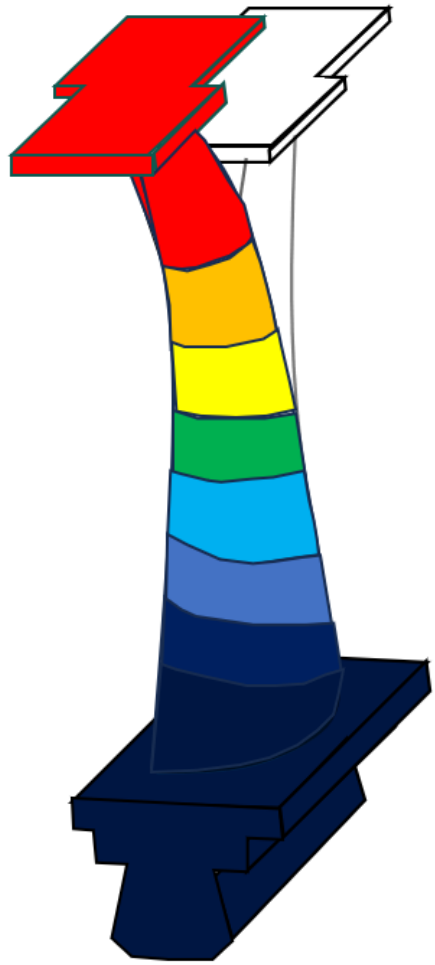

Figure 40: 1st Family Modeshapes - FLAP- TIP FREE CONFIGURATION

Figure 41: 1st Family Modeshapes - FLAP - TIGHT CONFIGURATION

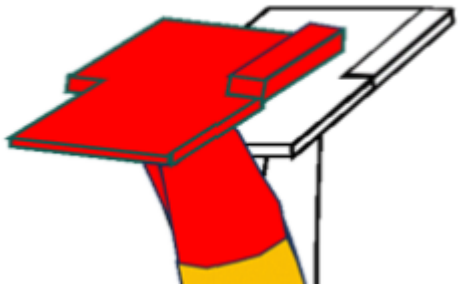

Figure 42: 1st Family Modeshapes - FLAP - RADIAL FREE CONFIGURATION

As the nodal diameters increase, the behavior of the RADIAL FREE and TIGHT configurations changes:

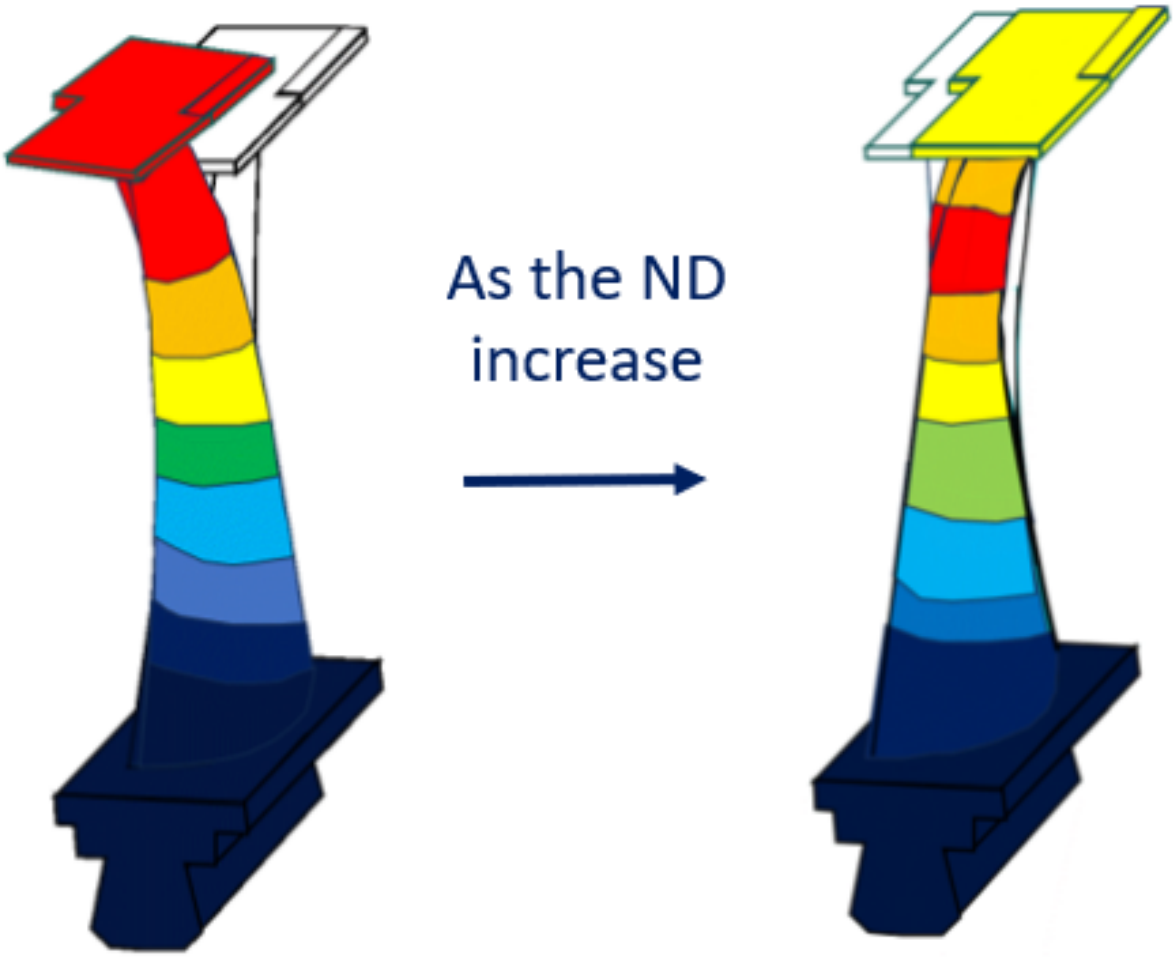

Figure 43: MODE TIGHT Configuration at the ND increase

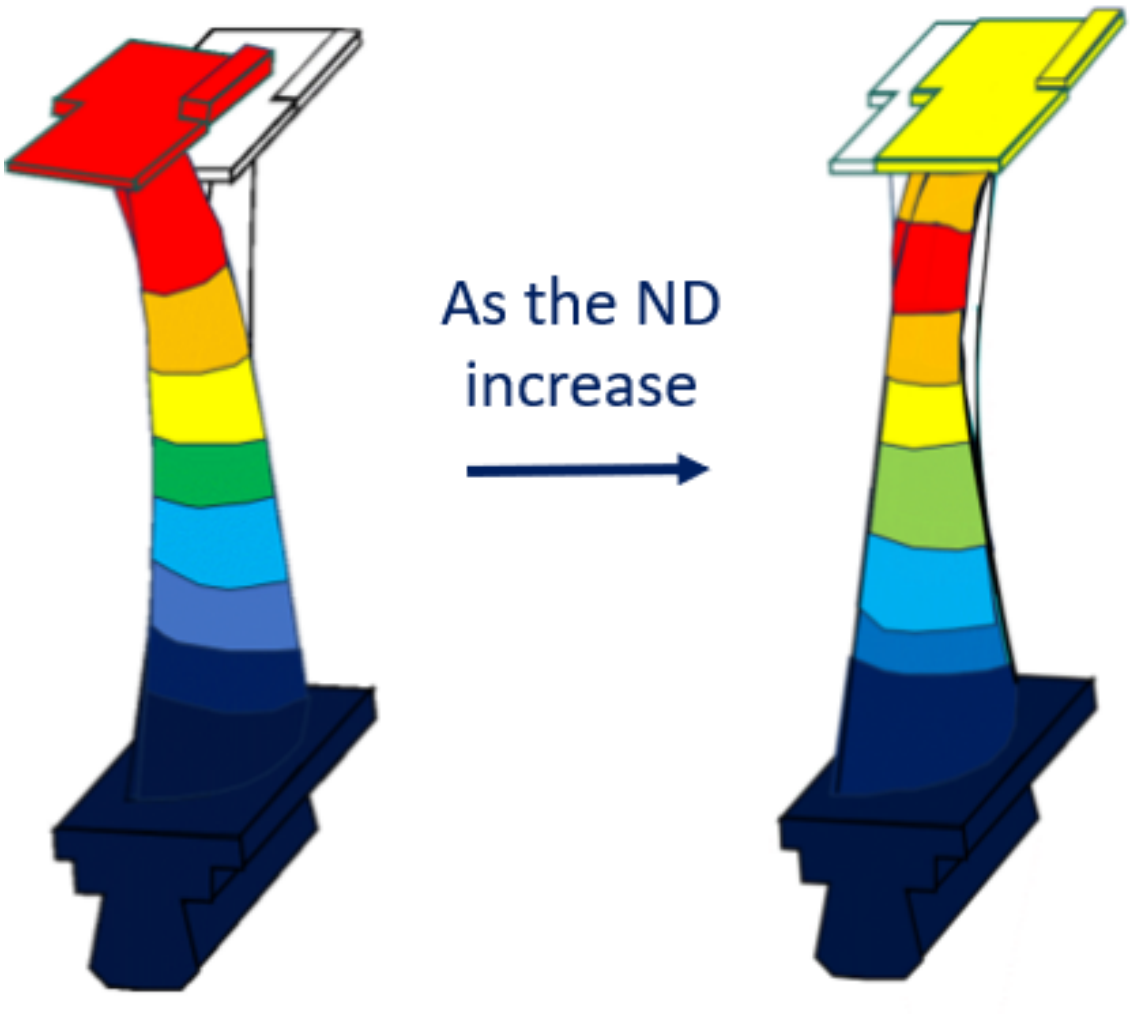

Figure 44: MODE RADIAL FREE Configuration at the ND increase

The maximum displacement zone moves in a lower one, it is possible to see the real effect of the constraint at the interlock.

The TIP FREE configuration, however, does not provide for a change in mode as the nodal diameters increase, the behavior of the blade remains similar to itself.

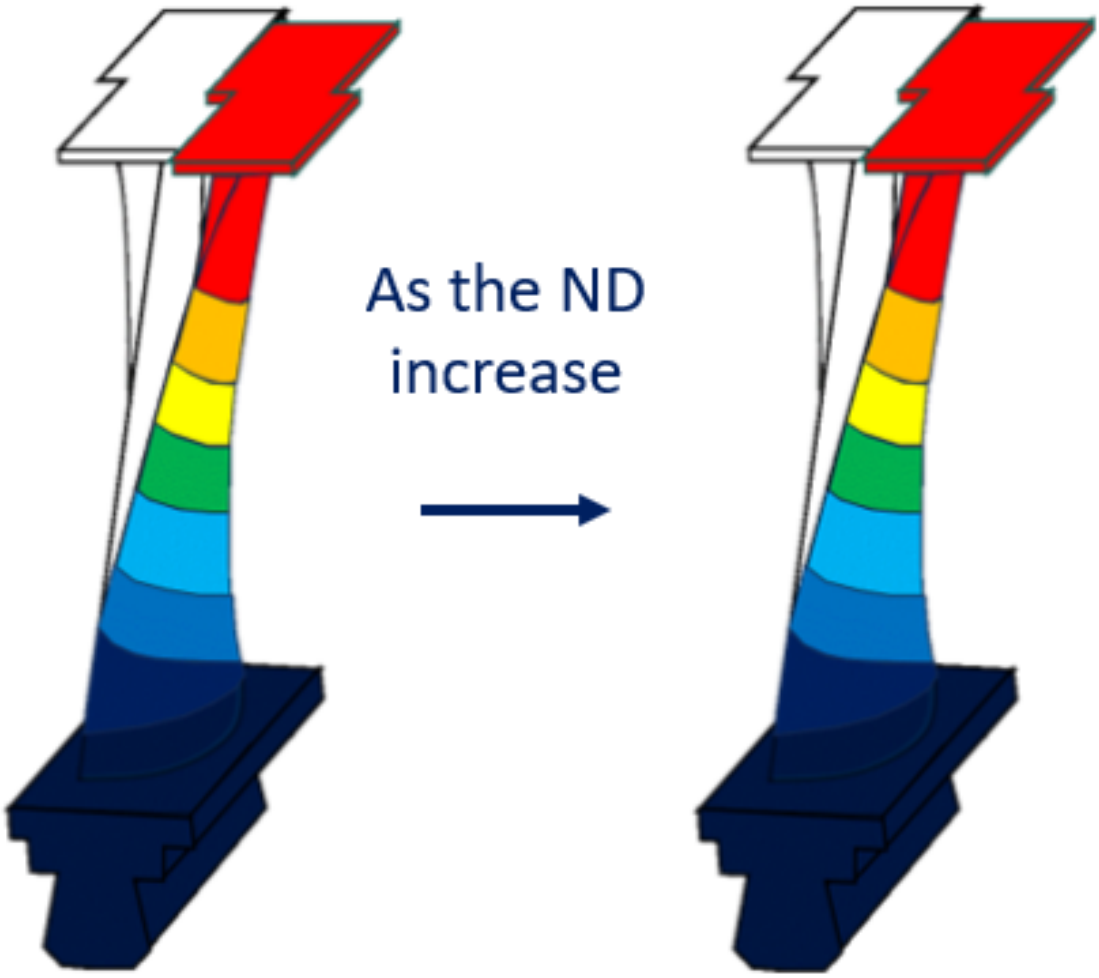

Figure 45: MODE TIP FREE Configuration at the ND increase

In the following figures are shown the freNDs of the Analysis.

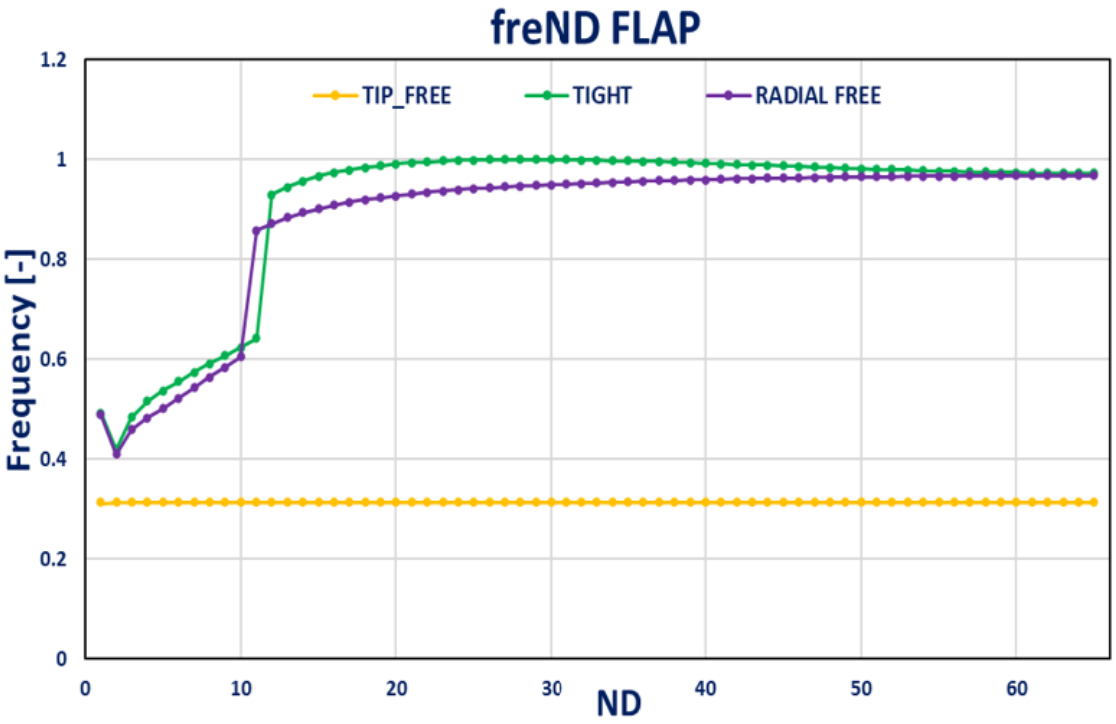

Figure 46: FreND by Frequency by Family FLAP

The different Interlocking Boundary Conditions affect the way the blade vibrates. In TIP FREE configuration, the blade moves by pure FLAP, but in the other two cases there is a weak torsional component that changes the way it vibrates.Moreover, the blade's behavior changes as the Nodal Diameters increase.

From the graphics it is possible to see that the TIP FREE frequencies is lower than the other two cases,the shroud gives the structure greater rigidity and in the TIP FREE configuration it is like having lost it, so it is as if the blade were cantilever. The analysis was also carried out for the second mode, the results of the aforementioned are reported: For the second mode the same considerations made for the first mode apply if it were not for the fact that the edge wise appears to be present only for the first nodal diameters as the mode then changes.

The analysis was also carried out for the second mode, the results of the aforementioned are reported:

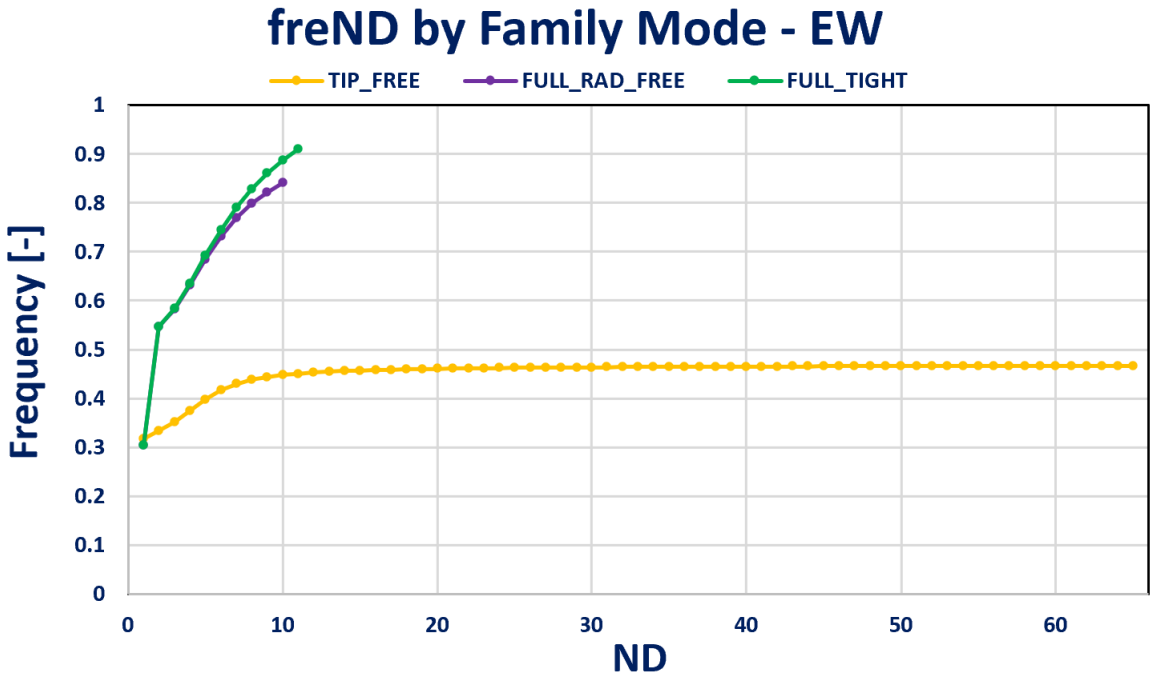

Figure 47: FreND by Frequency by Family EW

For the second mode the same considerations made for the first mode can be said if it were not for the fact that the Edge Wise mode appears to be present only for the first nodal diameters, the mode then changes.

5.2 CFD Steady State Analysis

To perform the Flutter Analysis the first step is to execute the CFD Steady State Analysis to initialize the flow. The Steady State Analysis refers to the condition where all the flow parameters do not change over the time throughout the entire domain.

Computational fluid dynamics (CFD) is a branch of fluid mechanics that uses numerical analysis and data structures to analyze and solve problems that involve fluid flows.To perform the CFD Analysis it is necessary to follow some steps:

- **Geometry**:It is necessary to define the geometry of the test study to visualize and define the flow domain and all the walls.
- **Mesh**: To perform the analysis the flow domain, so the volume is divided into discrete cells, the results of this division is called mesh.
- **Fluid Modeling** : The fluid must be modeling through some equations according to the analysis type that will be executed.
- **Boundary conditions**: It is necessary specify the fluid behavior around wall surfaces and bounding surfaces of the flow domain.

The CFD mesh used in this thesis work is a 3D grid mesh type H, this type of mesh is preferred for inter blades and in general for turbo-machine. It is also important to choose the *discretization methods*, in this case it was chosen the *finite volume method*.In this method the information is located in the cell.

$$\frac{\partial}{\partial t}\int_v u dV = -\int_s \overline{F}\cdot\ \overline{u} dS \tag{46}$$

$$\overline{u} = \int_V \frac{u dV}{V} \tag{47}$$

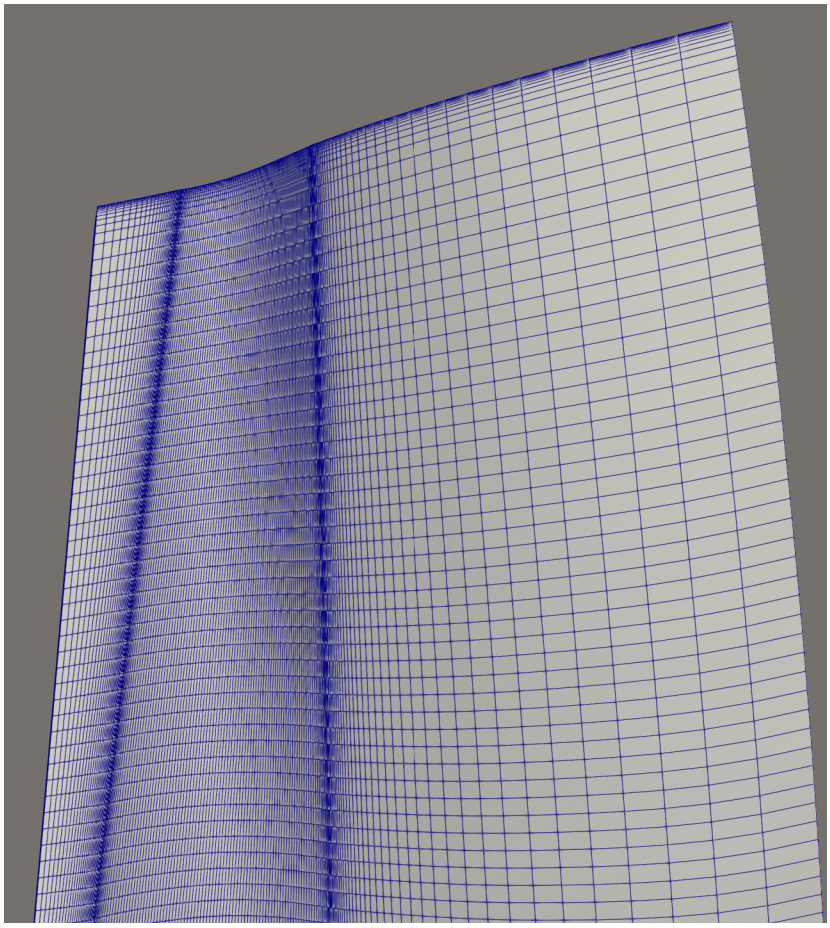

Figure 48: 3D grid mesh

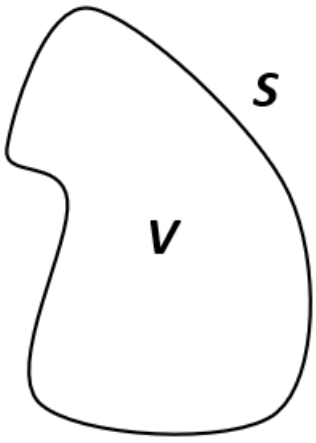

Figure 49: Generic cell

$$V\frac{\partial \overline{u}}{\partial t} = -\int_s \overline{F} \cdot \ \overline{u} dS \tag{48}$$

The unknown is the average of the velocity in every cells. It is necessary to evaluate the integral of the cell perimeter. What comes out of one cell enters the other, the flow at the interface is therefore calculated only once, this happens for continuity. To calculate the convective terms in the flows, upwind methods or centered methods can be used, for the present case an upwind method is used.

To model the flow, equations are needed that obviously describe it depending on the object of study or the characteristics of the phenomenon you want to study.
For *ideal and adiabatic flow* the Euler equations are used:

$$\begin{cases} \frac{\partial \rho}{\partial t} + \nabla \cdot \ (\rho \mathbf{u}) = 0 \\ \frac{\partial \rho \mathbf{u}}{\partial t} + \nabla \cdot \ (\rho \mathbf{u} \times \mathbf{u} + pI) = 0 \\ \frac{\partial E}{\partial t} + \nabla \cdot \ [\mathbf{u}(E + P)] = 0 \end{cases}$$

For *turbulent flows* are used three different approaches:

- **DNS** (*Direct Numerical Simulation*): is the most simple method but the computational cost is higher. With this approach I integrate the Navier-Stokes equations with a sufficiently fine grid, resolving the turbulence.
- **LES** (*Large Eddy Simulation*): only large scales are resolved, smaller scales are resolved with a model given their universality.

- **RANS** (*Reynolds Averaged Navier Stokes*): a Reynolds averaging operator is introduced, thus working with a mean field,it is the least reliable but most used method.

$$\begin{cases} \frac{\partial \rho}{\partial t} + \frac{\partial(\rho\overline{u_i})}{\partial x_i} = 0 \\ \frac{\partial(\rho\overline{u_i})}{\partial t} + \frac{\partial(\rho\overline{u_i u_j})}{\partial x_j} = -\frac{\partial \overline{p}}{\partial x_j} + \frac{\partial}{\partial x_j}\left[\mu\left(\frac{\partial \overline{u_i}}{\partial x_j} + \frac{\partial \overline{u_j}}{\partial x_i} - \frac{2}{3}\delta_{ij}\frac{\partial \overline{u_m}}{\partial x_m}\right)\right] + \frac{\partial}{\partial x_j}(-\rho\overline{u_i' u_j'}) \end{cases}.$$

At the base of the CFD analysis performed in this thesis work there is always the TRAF code. The code works with 5 main parameter, distributed between Inlet and Outlet.

- Inlet: $\alpha, \beta, p_1^{tot}, T_1^{tot}$
- Outlet:p_2

α and β are the absolute angles:

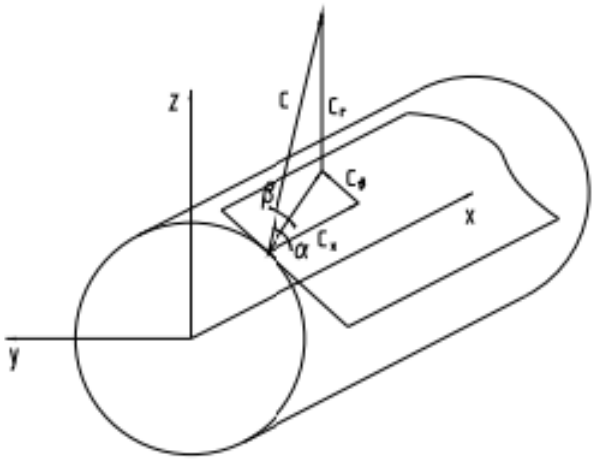

Figure 50: Absolute angles for a generic axial turbo-machine [9]

$$\alpha = arctan\frac{c_\theta}{c_x} \tag{49}$$

$$\beta = arctan\frac{c_r}{\sqrt{c_x^2 + c_\theta^2}} \tag{50}$$

Considering the number 1 for the Inlet and the number 2 for the outlet,for this work the Inlet and Outlet Condition are:

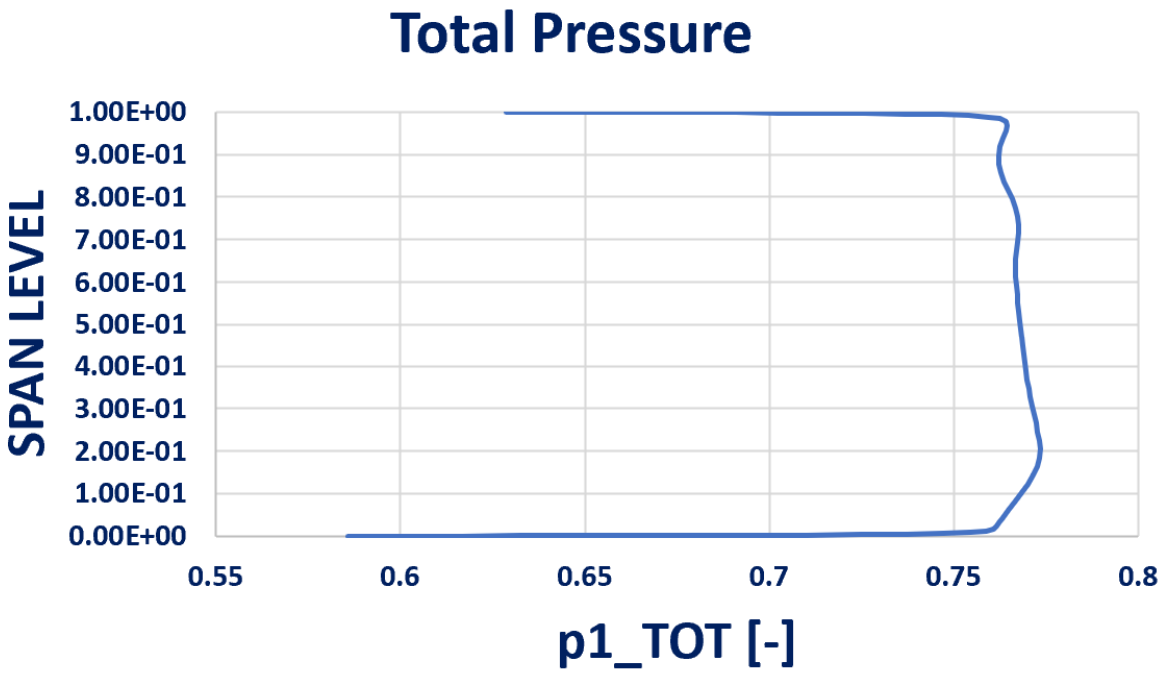

Figure 51: Total Pressure in Inlet

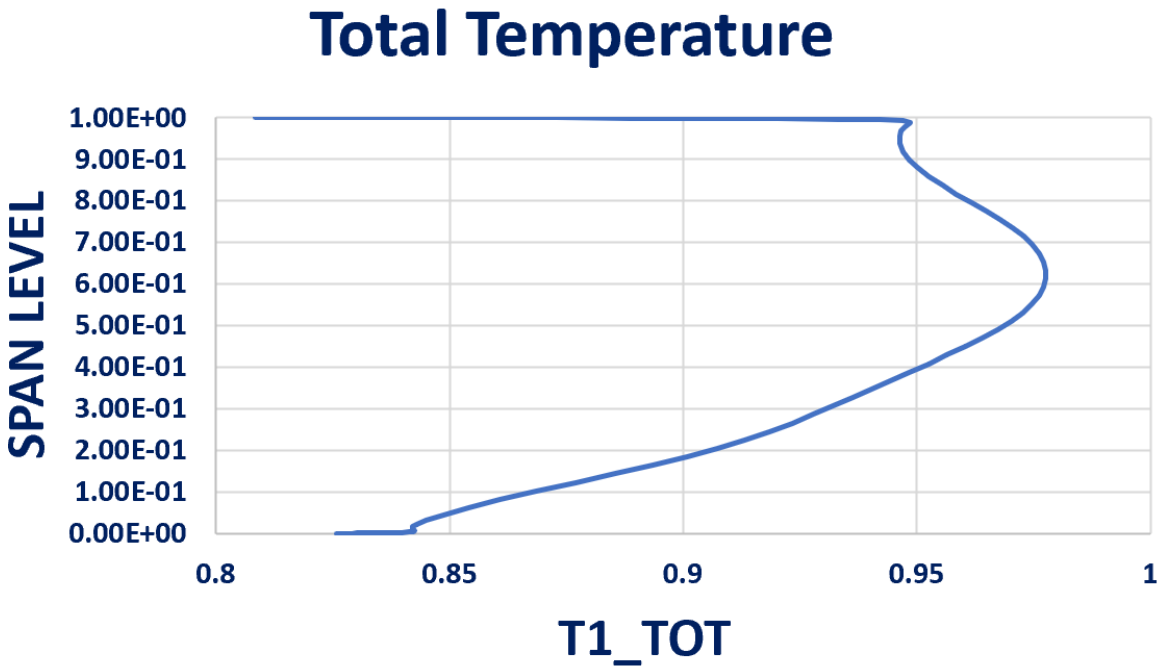

Figure 52: Total Temperature in Inlet

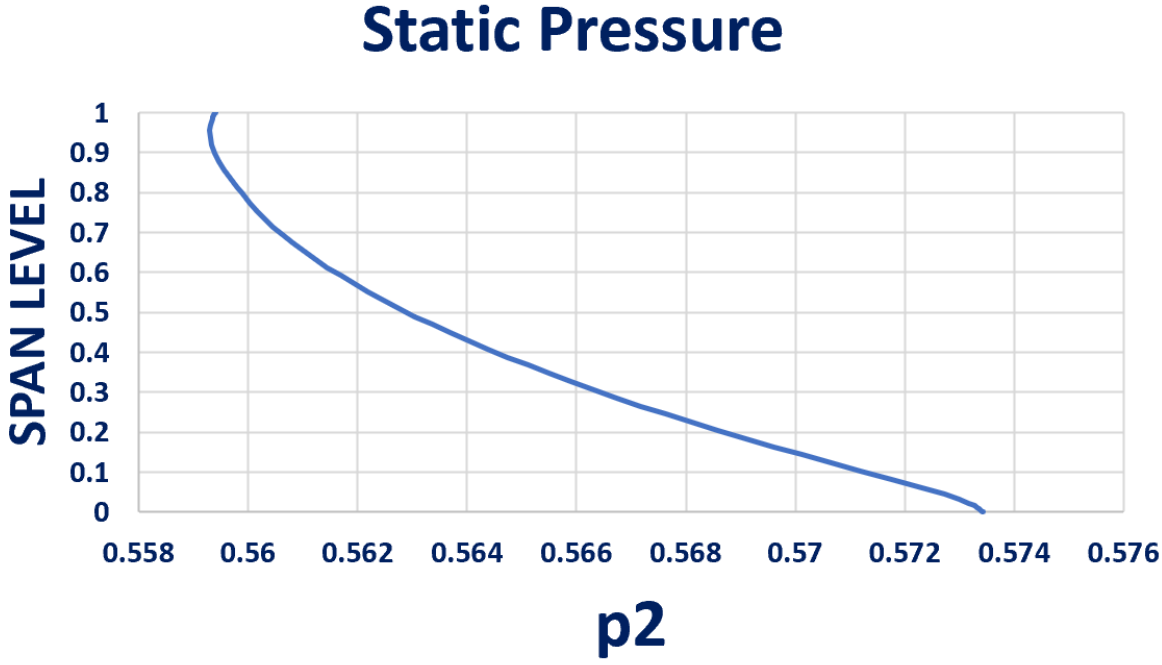

Figure 53: Static Pressure in Outlet

To be sure that the account has converged, plot the logarithm of the residual on the number of steps. If this drops significantly until it stabilizes, then the account has converged.

In the following figure is reported the convergence check of the CFD Analysis:

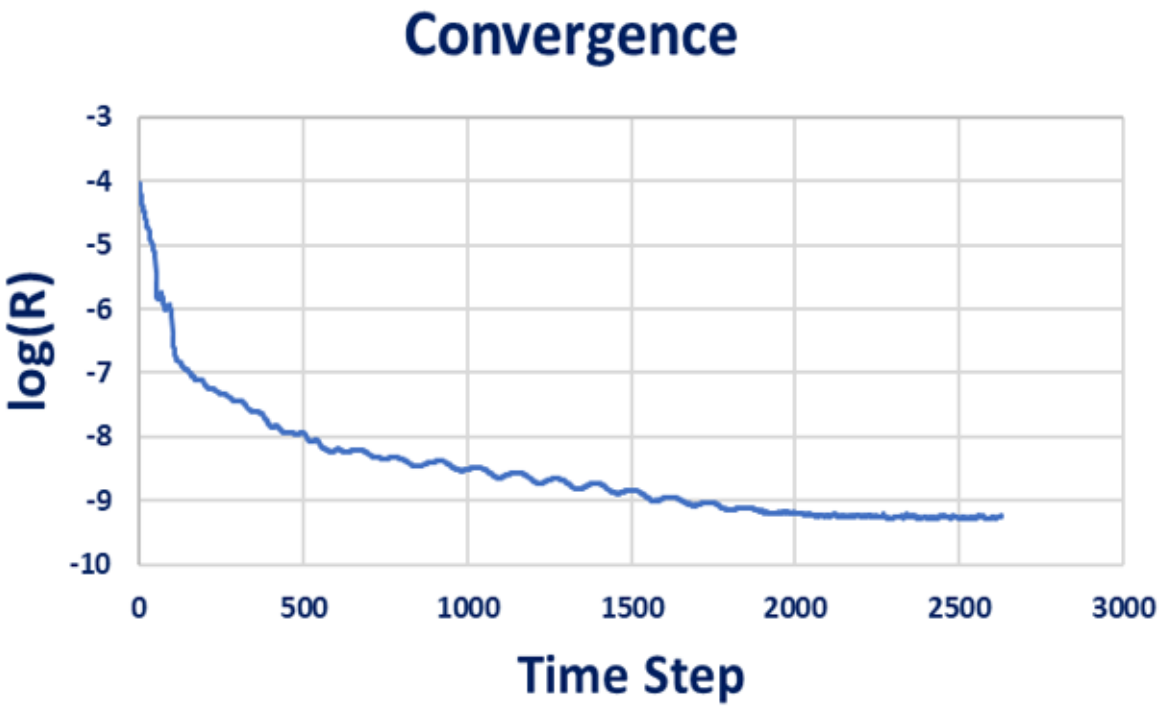

Figure 54: Convergence Check of the analysis

5.3 Grid Alignment

It is executed a Modal Analysis of the model, the solution is processed to obtain the modal displacements, witch are combined with the aerodynamic effects generated by the fluid. So there is a sharing between the aerodynamic effect obtained by the CFD SS and the Mechanic Effect obtained by the Modal Analysis.

The effects both must act simultaneously on the blade, so it is necessary doing the Grid Alignment to unify the two conditions.It is necessary to perform a mesh deformation strategies to allow the blade vibration during the simulation.

The alignment of the grids is carried out via CloudCompare. CloudCompare is a 3D point cloud (and triangular mesh) processing software (Open-Source). It has been originally designed to perform comparison between two dense 3D points clouds or between a point cloud and a triangular mesh.In this case it is used to compare and align the two grids.Three points are chosen on both grids, two at the hub and one at the tip to align the grids.

At the end of the alignment it is necessary to see the two grids well overlapped.

In the picture below there is an example of grid alignment,in white the FEM mesh and in pink the CFD mesh. It is necessary to have a good match between the two grids.

Figure 55: Grid Alignment

5.4 Flutter 3D Unsteady Analysis

Once all the above steps were completed, a Flutter 3D Unsteady Analysis was performed for each cases. In the picture below are shown the aero-plot,for reasons of company confidentiality, the ordinate axis is not shown:

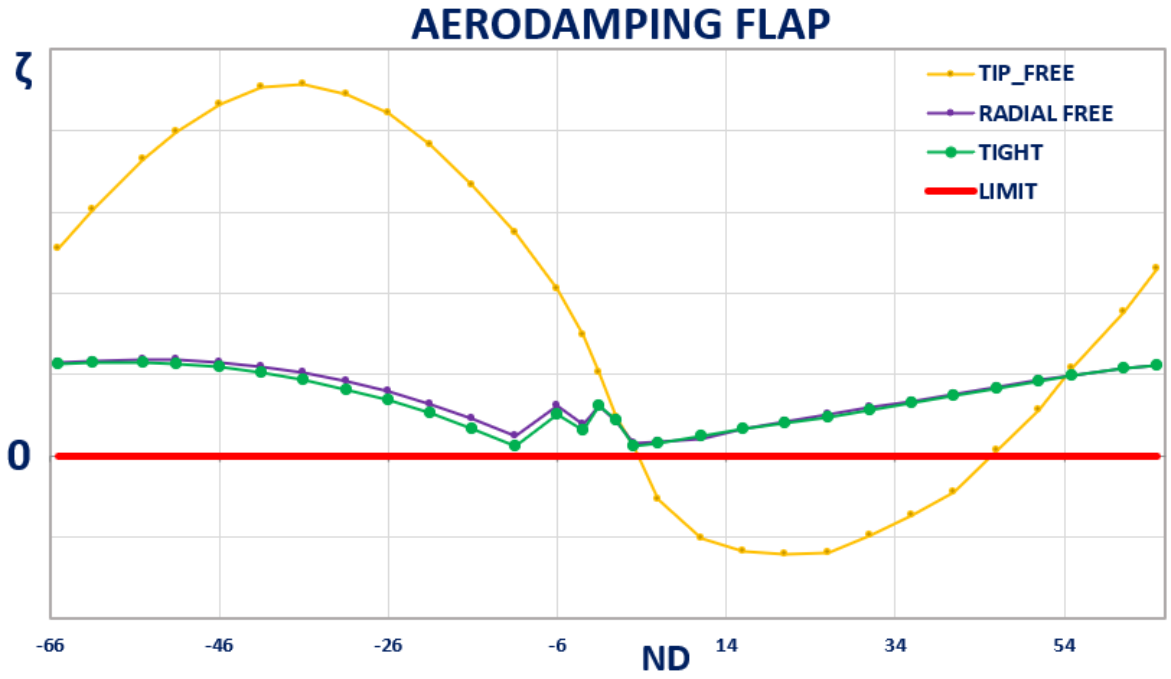

Figure 56: AEROPLOT FLAP Mode

It is also performed a Flutter Analysis for the second mode:

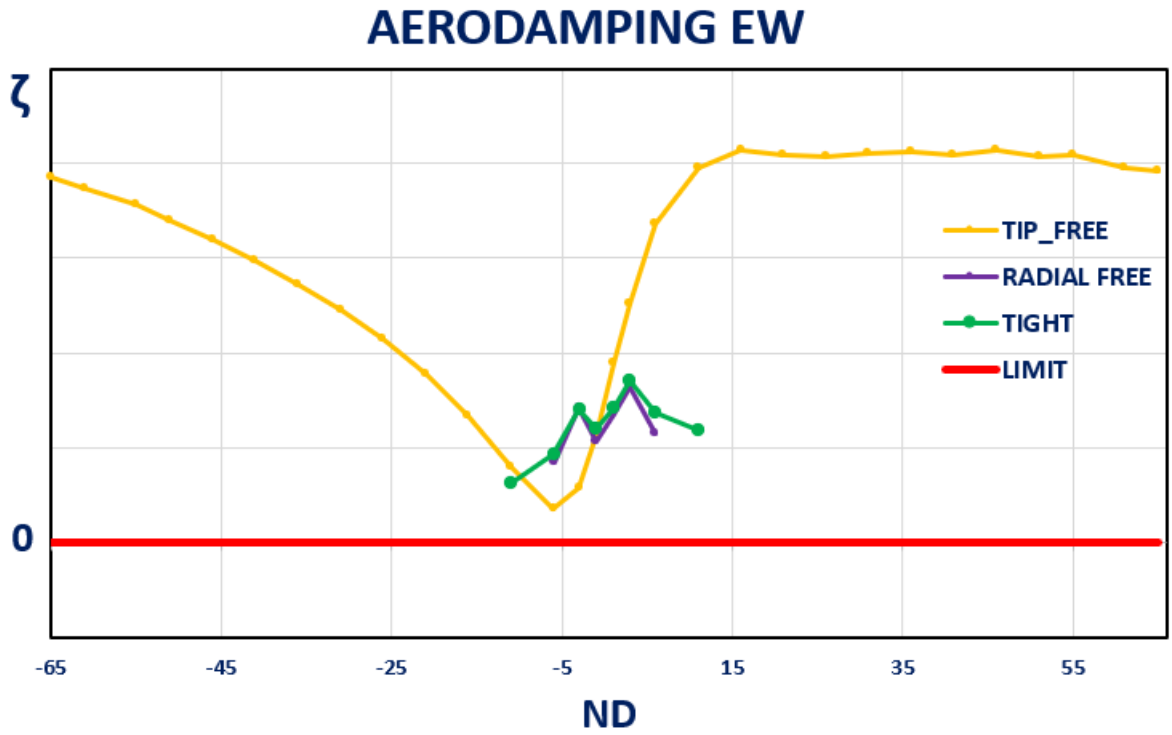

Figure 57: AEROPLOT EW Mode

From a quick look at the aeroplots it is possible to notice how the tip free for the first mode is unstable and the other two are always stable.The contact loss or the preload loss at the interlocking leads us to a condition of instability,the pressure field therefore tends to excite the flap mode, not dampening it but amplifying it, such as to create a self-sustained vibration, the aerodynamic work is positive so herefore, as we have already said, it carries out work on the structure, therefore flutter criticality. In the second mode all the configurations are stable, the EW mode don't allow us to a critic condition,this means that the pressure field does not excite the mode in any of the three configurations.

Focusing on the first mode, it is important to underline how the loss of the contact or the interlocking preload automatically leads us to a condition of flutter instability and therefore to a condition of extreme danger.

During the operational life of the component the contact could decrease or in any case the preload could disappear due to wear or material tolerances, the mode would therefore change instantly, putting us in a condition of extreme danger with the risk of breaking the component.

Each ordinate of the aeroplot, therefore each aerodamping value is the surface integral of the formula (44), which means that there is indeed a distribution along the aerodamping surface, there will therefore be parts of the airfoil that will dampen more and others less.

The 3D Flutter Analysis output also provides the distributions of aerodamping density, pressure amplitude and phase; in this regard, these distributions are shown for the most unstable nodal diameter,again for reasons of company secrecy the value scales will not be shown:

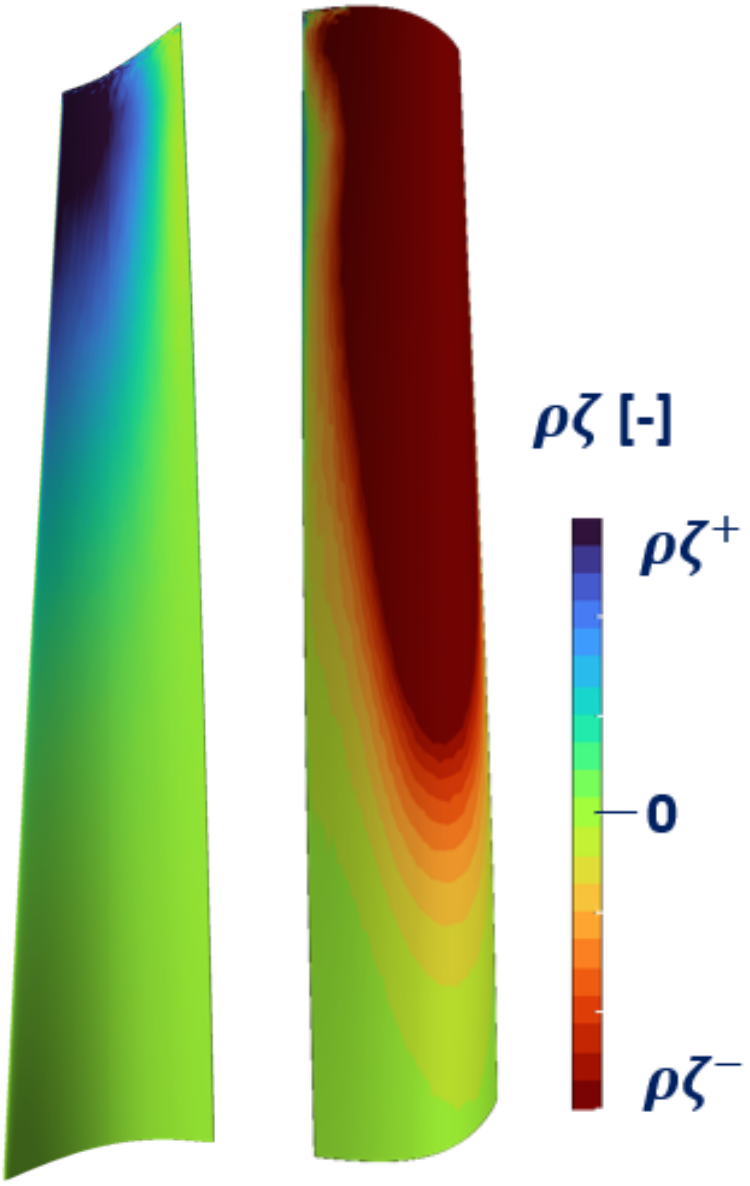

Figure 58: Aerodamping Density distribution

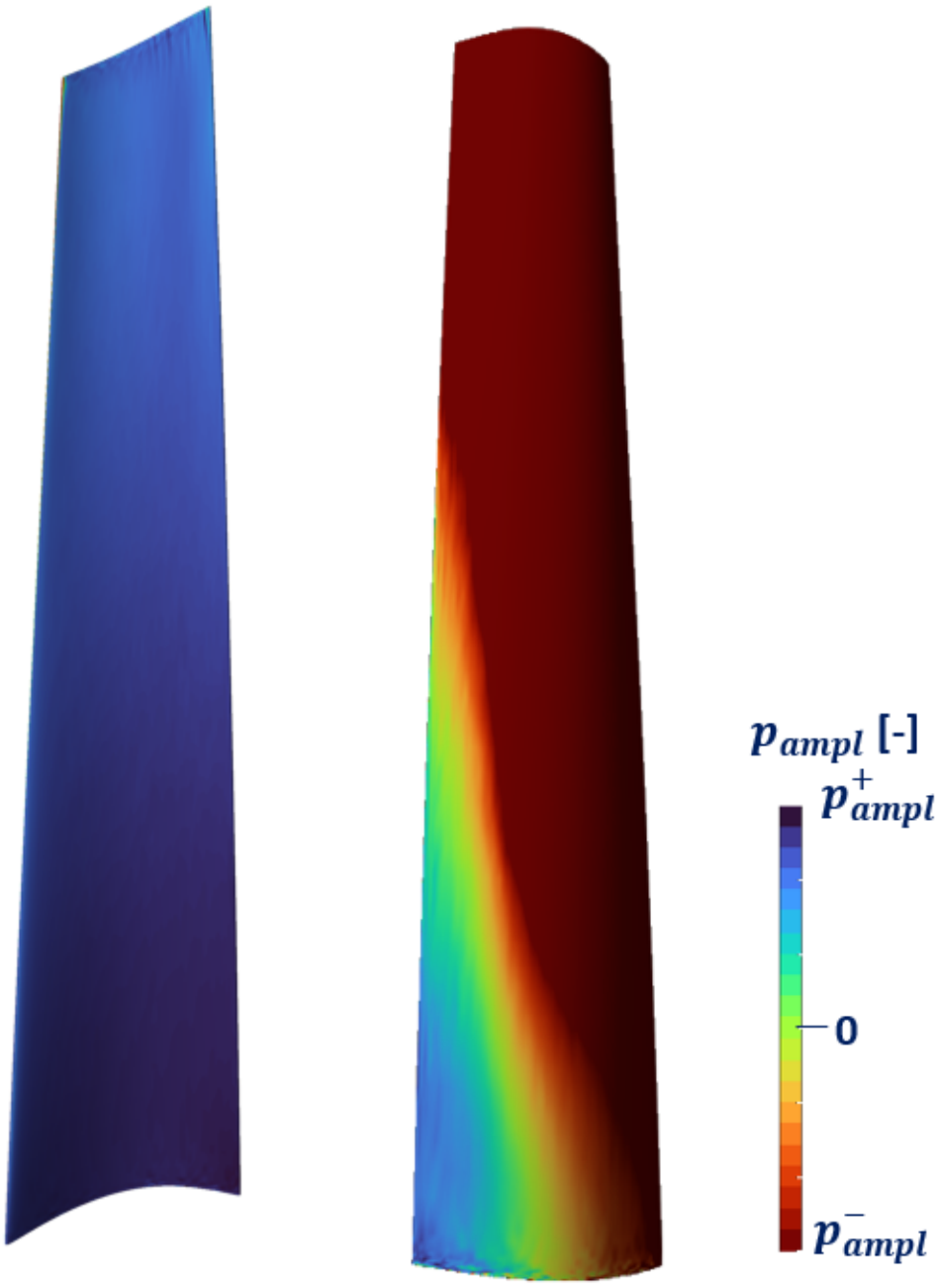

Figure 59: Pressure Amplitude Distribution

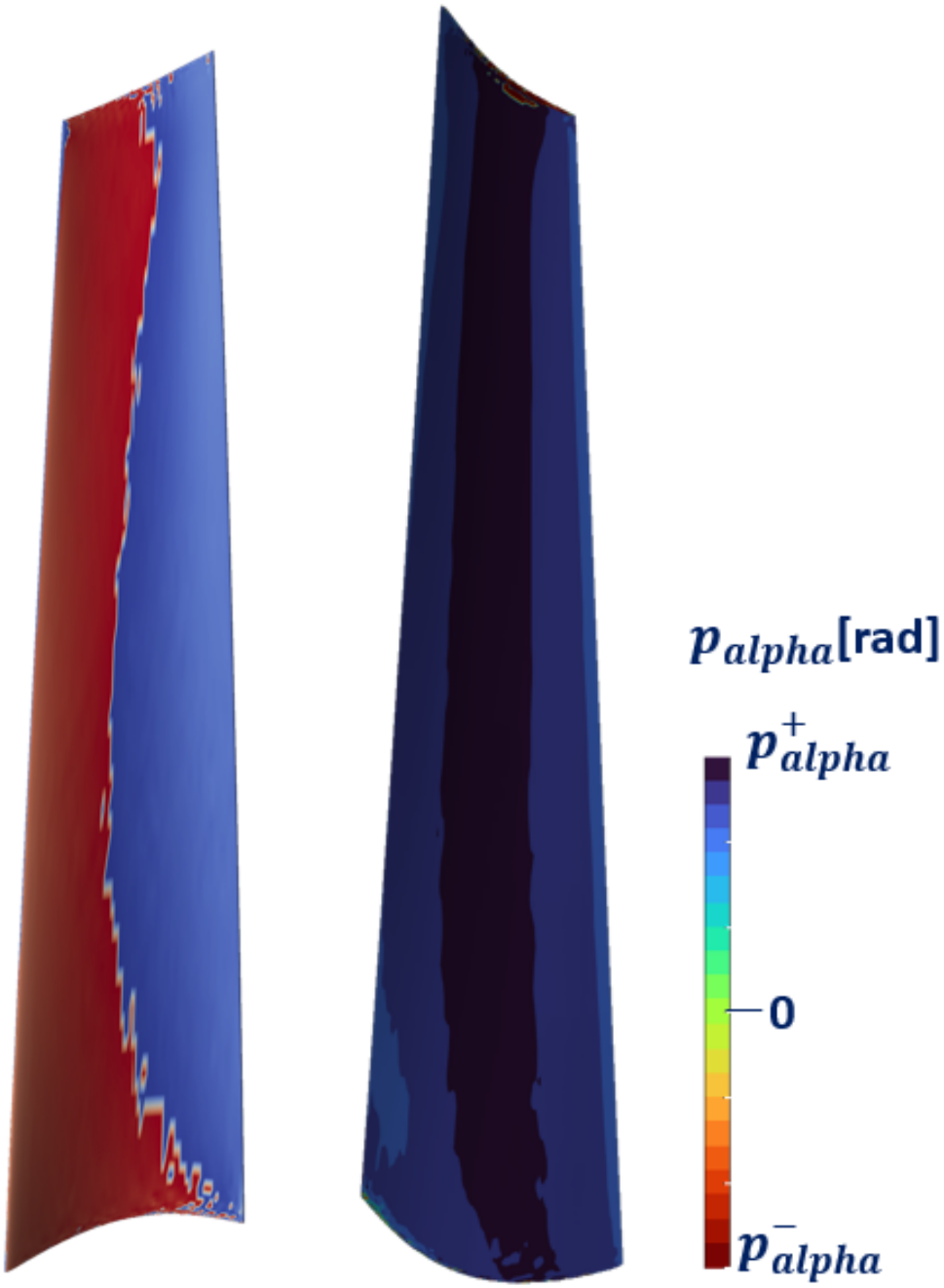

Figure 60: Pressure phase distribution

In the figures are represented the suction side and the pressure side both, but the first one respond most to flutter.
Looking at the suction side,as can be seen in figure [58], the zone of instability is very large, this is also reflected in the pressure amplitude in figure [59] where the high response can be seen and furthermore it can also be seen in figure [60] how the phase is positive. The zones of instability have a positive phase, whereas those of instability have a negative phase[10].

6 Conclusions

After presenting all the work done and the related results, it is time to draw the necessary conclusions.

The results show that the most important conclusion is the importance to simulate different types of contact to make sure to avoid flutter instability.When the blades are keyed on to the disk we do not know the type of contact that is generated at the interlocking and we also do not know if this contact will remain unchanged during the operational life of the component. Investigating the type of contact and its influence on an aeroelastic phenomenon such as flutter is crucial.In particular, it shows us that it is essential to simulate even the absence of contact, so it is legitimate to ask what impact the loss of preload has on flutter stability.

The contact type appears to have an influence on the frequency, the modes of vibration and the flutter stability.Losing the interlocking preload leads us to work at significantly internal frequencies, furthermore the way of vibration changes from one case to another, for the TIP FREE configuration this way of vibration remains similar to itself as the nodal diameters increase.The TIP FREE case, as seen from the results, appears to be unstable unlike the other two which are always stable.

From this it can be deduced that, for our case, the contact must not disappear to avoid flutter instability,so the tip free configuration must be prevent.

References

[1] E – TDCs Abstract. (2023)

[2] *A time – accurate 3D Method for turbomachinery blade flutter analysis, 12th International Symposium on Unstedy Aerodynamics.* Pinelli Lorenzo, Poli Francesco, Arnone Andrea, Schipani Claudia. (2009)

[3] *Aeroelastic investigation of turbine blade assemblies: cluster system and mistuned rows, 12th European Conference on Turbomachinery Fluid Dynamics and Thermodynamics.*F. Vanti, L. Pinelli, F. Poli, A. Arnone. (2017)

[4] Rolls Royce, *The jet engine*, Renault Printing Co Ltd, Birmingham, Fifth edition, 1996.

[5] Stefano Zucca, *Dinamica dei Rotori per Applicazioni Aerospaziali*, Dipartimento di Ingegneria Meccanica e Aerospaziale, Politecnico di Torino, , inedito, 2022.

[6] Roberto Marsilio, *Progetto di Motori per Aeromobili*, Dipartimento di Ingegneria Meccanica e Aerospaziale, Politecnico di Torino, , inedito, 2023.

[7] *Modal Assurance Criterion, Elsevier Ltd. Selection.* Miroslav Pastor, Michal Binda, Tomas Harcarik. (2012)

[8] *Z. Mazur – Czerwiec, A. Hernandéz – Rossette, R. Garcìa – Illesoas. (2006)* L – 0 blade flutter investigation of a 110 MW Geothermal Turbine, ASME 2006 Power Conference.

[9] *NOTES ON THE USE OF THE TRAF CODES. December 2021*,Andrea Arnone, Michele Marconcini Department of Industrial Engineer-

ing University of Florence.

[10] *THE ROLE OF OPERATING CONDITIONS ON FLUTTER INSTABILITY OF A LOW-PRESSURE TURBINE ROTOR* Lorenzo Pinelli, Francesco Poli, Andrea Arnone,Antonio Giuseppe D'Ettole, Emanuele Rosso, Gianmaria Sartor,Vsevolod Kharyton- Department of Industrial Engineering, University of Florence, Firenze, Italy;Avio Aero – a GE Aerospace company, Torino, Italy; Siemens Energy AB, Finspång, Sweden

[11] Valerio Piscopo, Analysis of Mulstistage Structures using Cyclic Symmetry, MSc thesis, Dipartimento di Ingegneria Meccanica e Aerospaziale, Politecnico di Torino, 2022.

[12] `https://en.wikipedia.org/wiki/Axialturbine`, Last Access April 2024.

[13] `https://it.wikipedia.org/wiki/File:Logo_Avio_Aero.jpg`

[14] `https://www.polito.it/`

[15] `https://en.wikipedia.org/wiki/Brayton_cycle`, Last Access March 2024.

[16] `https://en.wikipedia.org/wiki/Turbofan`, Last Access March 2024.

[17] `https://en.wikipedia.org/wiki/Turboprop`, Last Access March 2024.

[18] `https://en.wikipedia.org/wiki/Turbojet`, Last Access March 2024.

[19] `https://en.wikipedia.org/wiki/Axial_turbine`, Last Access

March 2024.

[20] https://www.geopop.it/tacoma-narrow-bridge-la-storia-del-ponte\
-che-crollo-dopo-soli-129-giorni/, Last access April 2024.

[21] https://www.parmadaily.it/7-novembre-1940-crollo-\
di-parte-del-tacoma-narrows-bridge/, Last access April 2024.

[22] hhttps://www.grc.nasa.gov/www/BGH/newton3.html,Last access March 2024.

[23] https://onlinelibrary.wiley.com/, Last Access April 2024.

[24] https://www.sciencedirect.com/topics/
physics-and-astronomy/modal-analysis:~:text=Modal,Last
Access May 2024.

[25] https://en.wikipedia.org/wiki/Computationalfluiddynamics,Last access April 2024.

[26] https://www.idealsimulations.com/resources/
turbulence-models-in-cfd/,Last Access April 2024.